

Clemson University

Clemson OPEN

All Theses

Theses

5-2026

Forest Overstory Mortality & Recruitment Patterns Eight Years Following Wildfire in the Southern Appalachians

Ruth Cumberland

Clemson University, ruth.cumberland@gmail.com

Follow this and additional works at: https://open.clemson.edu/all_theses



Part of the [Biodiversity Commons](#), [Botany Commons](#), [Forest Biology Commons](#), [Forest Management Commons](#), [Other Forestry and Forest Sciences Commons](#), and the [Terrestrial and Aquatic Ecology Commons](#)

Recommended Citation

Cumberland, Ruth, "Forest Overstory Mortality & Recruitment Patterns Eight Years Following Wildfire in the Southern Appalachians" (2026). *All Theses*. 4753.

https://open.clemson.edu/all_theses/4753

This Thesis is brought to you for free and open access by the Theses at Clemson OPEN. It has been accepted for inclusion in All Theses by an authorized administrator of Clemson OPEN. For more information, please contact kokeefe@clemson.edu.

FOREST OVERSTORY MORTALITY & RECRUITMENT PATTERNS EIGHT
YEARS FOLLOWING WILDFIRE IN THE SOUTHERN APPALACHIANS

A Thesis
Presented to
the Graduate School of
Clemson University

In Partial Fulfillment
of the Requirements for the Degree
Master of Science
Wildlife & Fisheries Biology

by
Ruth Margaret Cumberland
May, 2026

Accepted by:
Dr. Don Hagan
Dr. Troy Farmer
Dr. Lillie Lnglois

PLAIN LANGUAGE ABSTRACT

In this study, we investigated patterns of forest overstory mortality and recruitment eight years after wildfire at a large wildfire site in the Southern Appalachians, a topic that has not been thoroughly investigated to date. With evidence that pre-fire drought promotes post-fire mortality through impaired physiological function and increased fuel consumption, unknown patterns following wildfire are important to study under shifting climate and land-use conditions. In Chapter 1, three areas of forest overstory mortality response to the 2016 wildfire events were investigated: (a) functional group response, (b) temporal differences in early (1-3 years) and late (5-8 years) periods, and (c) solar radiation and topographical variation influences to cumulative mortality. Analyses revealed: (a) fire-adapted overstory species were most resistant to wildfire effects, followed by heath species, then fire-sensitive species; (b) mortality hazard risk increases in the later periods after wildfire than the early periods for all species of interest; and (c) cumulative mortality over eight years showed that wildfire-induced mortality odds increase significantly from wetter, cooler sites to drier, warmer sites. In Chapter 2, research investigated forest regeneration response eight years post-fire. Non-metric multidimensional scaling and generalized linear mixed effects models assessed functional group responses of differing plant communities. Findings suggest that a single drought-induced wildfire in the southern Appalachians may accelerate mesophication, with the strongest effects in Thermic Oak Forests, indicating a potential ecological resilience debt in long-unburned plant communities of the southeast.

ABSTRACT

In this study, we investigated patterns of forest overstory mortality and recruitment eight years after wildfire in a large wildfire site the Southern Appalachians, a topic that has not been thoroughly investigated to date. With evidence that pre-fire drought promotes post-fire mortality through impaired physiological function and increased fuel consumption, unknown patterns following wildfire are important to study under shifting climate and land-use conditions. In Chapter 1, three areas of interest were investigated: (a) functional group mortality response to wildfire effects, (b) temporal differences in early (1-3 years) and late (5-8 years) periods of delayed forest overstory mortality patterns following wildfire, and (c) solar radiation and topographical variation influences to cumulative forest overstory mortality. Analyses revealed: (a) fire-adapted overstory species were most resistant to fire effects, followed by heath, then fire-sensitive species. (b) mortality hazard risk increased in the later period compared to the early period, and (c) cumulative mortality over eight years showed that fire-induced mortality odds increased significantly from mesic sites to xeric sites. In Chapter 2, research addressed forest regeneration response eight years post-fire. Non-metric multidimensional scaling and generalized linear mixed effects models assessed functional group responses of differing plant communities. Findings suggest that a single drought-induced wildfire in the southern Appalachians may accelerate mesophication, with the strongest effects in Thermic Oak Forests, indicating a potential ecological resilience debt in long-unburned and fire-maintained plant communities of the southeast.

TABLE OF CONTENTS

	Page
TITLE PAGE	i
PLAIN LANGUAGE ABSTRACT.....	ii
ABSTRACT.....	iii
LIST OF TABLES	vii
LIST OF FIGURES	ix
CHAPTER ONE: DELAYED FOREST OVERSTORY MORTALITY IN THE	
SOUTHERN APPALACHIANS FOLLOWING WILDFIRE.....	1
Introduction.....	1
Methods.....	6
Results.....	19
Discussion.....	30
Literature Cited	35

CHAPTER TWO: FOREST REGENERATION PATTERNS FOLLOWING

WILDFIRE IN THE SOUTHERN APPALACHIANS 46

 Introduction..... 46

 Methods..... 49

 Results..... 57

 Discussion..... 65

 Literature Cited 69

 Appendix A..... 80

 Appendix B..... 86

LIST OF TABLES

Table		Page
1.1	Mortality statistical summary by group and treatment at rock mountain wildfire site in Chattahoochee National Forest, Georgia, USA.....	20
2.1	Regeneration density (stems/ha \pm SE) by species group and treatment at rock mountain wildfire study site in Chattahoochee National Forest, Georgia, USA.....	61
A1	Posterior estimates of fire effects on overstory mortality by functional group from Bayesian hierarchical logistic regression (Model 1).....	80
A2	Posterior estimates of interaction effects from Bayesian hierarchical logistic regression (Model 1).....	80
A3	Model 2 raw mortality rates by period and treatment at rock mountain, 2016... ..	81
A4	Model 2-predicted mortality hazard rates by period and treatment from Bayesian hierarchical logistic regression (Model 2).....	82
A5	Fire effect on mortality hazard by period from Bayesian hierarchical logistic regression (Model 2).....	82
A6	Model 2 parameter estimates from Bayesian hierarchical logistic regression.....	83

List of Tables (Continued)

Table		Page
A7	Model-predicted mortality probability (%) across heat load index (HLI) sites from Bayesian hierarchical logistic regression (Model 3).....	84
A8	Fire effect on mortality across the topographic moisture gradient from Bayesian hierarchical logistic regression (Model 3).....	84
A9	Model 3 parameter estimates from Bayesian hierarchical logistic regression.....	85
B1	Post-hoc pairwise contrasts results of regeneration density at rock mountain study site.....	86
B2	Post-hoc pairwise contrasts results of regeneration relative abundance at rock mountain study site.....	87

LIST OF FIGURES

Figure	Page
1.1	Study area map showing the Rock Mountain Wildfire perimeter (black) in Chattahoochee National Forest, Georgia, & Nantahala National Forest, North Carolina, USA. Federal Lands are denoted in green.....6
1.2	Plot diagram of second hierarchy used in data collection at Rock Mountain Wildfire. First hierarchy level trees assigned as lowest level observational unit for forest overstory mortality data collection methods at Rock Mountain Wildfire site in Chattahoochee National Forest, Georgia, USA. Data collected in 2017, 2018, 2019, 2020, 2021, and 2024.....8
1.3	Heat Load Index (HLI), an index that displays diffuse and direct solar radiation on site in conjunction with slope, aspect, and elevation, fixed per hemisphere (McCune & Keon 2002). HLI on site was calculated and subsequently symbolized by the Natural Breaks (Jenks) method. Displayed are a subset of plots at The study site where HLI values were extrapolated for use as a covariate. Cooler topography denotated by blue, moderate by white, and warmer, drier, xeric by red..... 10
1.4	Percent overstory mortality by functional group and fire treatment from Bayesian hierarchical logistic regression using a binomial likelihood and logit link. Analysis was based on individual tree survival status of eight years post-treatment across burned and unburned plots. Light bars represent predicted mortality rates (%) in unburned control plots; dark bars represent plots burned in the 2016 Rock Mountain Fire. Error bars indicate ± 1 SE of posterior mean estimates. Odds ratios (OR) indicate the change in mortality odds for burned

List of Figures (Continued)

Figure	Page
<p>versus unburned conditions within each functional group. Asterisks denote effects where 95% credible intervals exclude 1.0. Pyrophytic group: <i>Quercus montana</i>, <i>Q. coccinea</i>, <i>Q. alba</i>, <i>Q. velutina</i>, <i>Q. rubra</i>, <i>Q. falcata</i>; Pyrophobic group: <i>Acer rubrum</i>, <i>Liriodendron tulipifera</i>; Heath group: <i>Oxydendrum arboreum</i>.....</p>	20
<p>1.5 Forest plot of fire effects on overstory mortality by group from Bayesian hierarchical logistic regression (Model 1). Points represent posterior mean estimates of fire effects on the log-odds scale; horizontal lines indicate 95% credible intervals. The vertical dashed line at zero represents no effect; values to the right indicate increased mortality in burned plots relative to unburned controls. Asterisks denote effects where 95% credible intervals exclude zero.....</p>	21
<p>1.6 Percent overstory mortality by functional group and fire treatment from Bayesian hierarchical logistic regression using a binomial likelihood and logit link. Analysis was based on individual tree survival status of eight years post-treatment across burned and unburned plots. Light bars represent predicted mortality rates (%) in unburned control plots; dark bars represent plots burned in the 2016 Rock Mountain Fire. Error bars indicate ± 1 SE of posterior mean estimates. Odds ratios (OR) indicate the change in mortality odds for burned versus unburned conditions within each functional group. Asterisks denote effects where 95% credible intervals exclude 1.0. Pyrophytic group: <i>Quercus montana</i>, <i>Q. coccinea</i>, <i>Q. alba</i>, <i>Q. velutina</i>, <i>Q. rubra</i>, <i>Q. falcata</i>; Pyrophobic group: <i>Acer rubrum</i>, <i>Liriodendron tulipifera</i>; Heath group: <i>Oxydendrum arboreum</i>.....</p>	23

List of Figures (Continued)

Figure		Page
1.7	Temporal patterns of overstory mortality hazard from Bayesian survival analysis. Points represent posterior mean hazard rates ($\pm 95\%$ credible intervals) for early (1–3 years) and late (5–8 years) post-fire periods. Light symbols indicate unburned control plots; dark symbols indicate plots burned in the 2016 Rock Mountain Fire. Increasing hazard in both treatments with persistent fire effects suggests continued delayed mortality eight years post-fire.....	24
1.8	Predicted mortality probability across the topographic Heat Load Index from Bayesian hierarchical logistic regression. Heat Load Index (HLI) represents potential solar radiation, with higher values indicating xeric southwest-facing slopes. Points show posterior mean estimates at mesic, intermediate, and xeric positions for unburned (light) and burned (dark) plots following the 2016 Rock Mountain Wildfire.....	25
1.9	Forest plot of key parameters from Bayesian hierarchical logistic regression, Model 3. Points represent posterior mean log-odds estimates, horizontal lines = 95% credible intervals, and the vertical line = line of no effect. Heat Load Index (HLI) represents potential solar radiation impact on soil moisture. The HLI \times Fire interaction tests whether fire effects vary across solar radiation and topographic influence. Asterisks = 95% credible intervals excluding zero.....	26

List of Figures (Continued)

Figure		Page
2.1	Plot diagram of 3x3 m observational units used in data collection at Rock Mountain Wildfire site in Chattahoochee National Forest, Georgia, USA. Data collected in 2024.....	47
2.2	Shepard plot for two-dimensional (k=2) non-metric multidimensional scaling ordination showing observed Bray-Curtis dissimilarities versus ordination distances. Stepped line represents the non-metric fit and the dashed line represents linear fit.....	55
2.3	Results of non-metric multidimensional scaling ordination of overstory trees at Rock Mountain using a Bray-Curtis dissimilarity distance measure. Analysis was based on genus-level relative abundance in each plot. Gray symbols are unburned plots and orange symbols are burned plots. Circles represent Bottomland/Cove communities, squares represent Mid-slope Oak/Pine communities, and triangles represent Thermic Oak/Oak-Pine communities. Arrows represent species vectors showing direction and magnitude of increasing abundance: solid arrows indicate pyrophytic species, dashed arrows indicate pyrophobic species, and dotted arrows indicate heath species. Final stress for the two-dimensional solution was 0.115.....	56
2.4	Regeneration density by species group and plant community following the 2016 Rock Mountain Fire. Closed circles represent unburned plots and open circles represent burned plots. Points show mean density ($\pm 95\%$ CI). Pyrophobic species show statistically significantly elevated regeneration in burned Mid-slope Oak/Pine and Thermic Oak communities (** $p < 0.001$), while pyrophytic regeneration did not differ by treatment.....	60

List of Figures (Continued)

Figure		Page
2.5	Relative abundance of regeneration by functional group and plant community following the 2016 Rock Mountain Fire. Closed circles represent unburned plots, open circles represent burned plots. Points show mean relative abundance ($\pm 95\%$ CI). Fire significantly decreased pyrophytic dominance in Thermic Oak communities and pyrophobic relative abundance was significantly elevated in burned Mid-slope and Thermic Oak sites. Note: *** $p < 0.001$	61
A1	Forest plot of Model 1 coefficients relative to pyrophytes. Points represent posterior mean log-odds estimates, horizontal lines indicate 95% credible intervals, and the vertical line= line of no effect. Circles = main effects, triangles = group intercepts, squares = Fire \times Group interactions, diamonds = covariates. Asterisks = 95% credible intervals excluding zero.....	77

CHAPTER ONE: DELAYED FOREST OVERSTORY MORTALITY PATTERNS
FOLLOWING WILDFIRE IN THE SOUTHERN APPALCHIANS

INTRODUCTION

The southern Appalachian Blue Ridge Mountains are secondary forests characterized by their high biodiversity, ancient geologic formation, temperate climate, and ecological changes undergone in the 21st century that included widescale logging, invasive species infestation, and change of ecological disturbance regimes (Flatley et al., 2013; Yarnell, 1998). Fire, a historical ecological disturbance regime, shaped Southern Appalachian forests with fire return intervals of two to 19 years pre-fire suppression and exclusion policy (Flatley et al., 2013; Lafon et al., 2017). Since the onset of these policies in the 21st century, fire events have been less common yet have increased in the early 1980's, burning less than 1,000 hectares on average annually until the 2016 fire events. These fires burned more than 70,000 hectares- more area than the previous three decades combined, and the majority of which burned in an approximately six-week timeframe (Reilly et al., 2022a).

Current Southern Appalachian forests are shaped by an overlap of climate, fire history, land use, species composition, and topographic complexity, yet long-term consequences of wildfire on forest dynamics remain poorly understood. While delayed post-fire mortality has been studied extensively in western United States forests, few studies have examined forest overstory mortality dynamics beyond four years post-fire in

the Southern Appalachians. This study addresses three interconnected knowledge gaps to provide a foundation to continue research over time: (1) whether pyrophobic species experience disproportionately higher cumulative delayed mortality than pyrophytic or heath species following drought-induced wildfire, reflecting the mesophication dynamic that has reshaped Southern Appalachian forest composition under long-term fire exclusion; (2) whether mortality risk increases in the years five through eight post-fire, indicating delayed physiological effects beyond the window typically captured; and (3) whether xeric topographic conditions, through increased solar radiation exposure, amplifies delayed overstory mortality. Together, these questions address a gap in knowledge regarding how long-term forest structure and composition are shaped in a region where fire regimes are projected to intensify under climate change.

Prior to the 2016 fire events, the region went through a period of extreme drought leading to favorable conditions for an active wildfire season. Severe drought conditions favor high values of the Keetch-Byram Drought Index (KBDI), an index used to measure soil moisture and cumulative moisture deficit on a scale from 0-800 (Keetch and Byram, 1968) and aids in assessing drought conditions to the topmost layers of soils. High KBDI values (600-800), the values of the 2016 fire events, are associated with fires that can consume the organic horizon where ectomycorrhizal (ECM) fine roots concentrate (Carpenter et al., 2021; Keetch and Byram, 1968). In addition to high KBDI, the 2016 fires were categorized as mostly low to moderate intensity flame lengths with smoldering combustion, duff consumption, and fine root elimination (Carpenter et al., 2021; Reilly et al., 2022b).

In western United States forests, delayed forest overstory mortality can continue for five to seven plus years post fire (Hood et al., 2018). While many forest mortality studies after wildfire have assessed either immediate or two to four years post-fire mortality (Abella et al., 2021; Cansler et al., 2024; Hood et al., 2018), few have studied five to seven plus years post-fire in the Southern Appalachians (Reilly et al., 2022b). Delayed mortality is particularly pronounced in larger trees of long-unburned forests, where smoldering combustion and cambium damage gradually disrupt xylem and phloem function, with physiological decline progressing over time (Hood, 2010; Hood et al., 2018). Although thick bark limits heat conduction to vascular tissues, prolonged smoldering may impair water and nutrient uptake through fine root loss and mycorrhizal disruption in the soil (Carpenter et al., 2021; Hood et al., 2018). Trees already experiencing high climatic water deficits prior to fire face increased mortality risk, as pre-fire drought further impairs physiological function and increases fuel consumption (Cansler et al., 2024; van Mantgem et al., 2013).

On xeric, southwest-facing slopes, higher solar radiation increases soil temperatures by up to five degrees Celsius; where fuels are more likely to ignite and combust compared to northeast-facing slopes (McCune and Keon, 2002; Seyfried et al., 2021), potentially intensifying belowground heat damage during smoldering combustion. In western forests, the resulting fine root loss can initiate a decline spiral where reduced water and nutrient uptake and the capacity to repair fire damage, making them more susceptible to mortality from other stressors, like insects and disease (Hood and Bentz, 2007; Hood et al., 2018; Kolb et al., 2016; Robbins et al., 2022).

Drought and fire interactions are projected to intensify under climate change. Robbins et al. (2024) modeled future fire regimes in the Southern Appalachians and found total burned area may increase by 42 to 105 percent by year 2100 for various drought severity scenarios, with higher projections indicating approximately 80,000 hectares burning annually, approximately equivalent to the 2016 wildfire footprint (Reilly et al., 2022b; Robbins et al., 2022).

In a paper by Nowacki and Abrams (2008), the ecological phenomenon of *mesophication* is described as the gradual replacement of fire-adapted species with shade-tolerant and fire-sensitive species leading to compositional and structural shifts. The shift in forest composition creates a positive feedback loop for fire-adapted species to more shade-tolerant or mesophytic species, especially after long-term fire exclusion (Hart et al., 2012). Although the oak-fire hypothesis suggests fire promotes fire-adapted and dependent species, emerging scientific discussion suggests the reintroduction of fire in fire-suppressed landscapes may play a role in accelerating mesophication (Carpenter et al., 2021; Reilly et al., 2022b)

Objectives of this study are to assess research gaps of delayed forest overstory mortality following wildfire in southeastern US forests. Although there has been detailed literature on delayed forest overstory mortality in the western United States, in the Southern Appalachians, there remains limited research specifically as it pertains to patterns among mesophytic functional groups, temporal patterns, and topographic position. With a changing climate, current land use patterns, and current policy practices, understanding

forest structure and composition are important for predicting long-term ecosystem responses and informing forest management decisions. Our hypotheses are as follows: 1) Fire-intolerant (Pyrophobic) species will show greater cumulative delayed forest overstory mortality than fire-adapted (Pyrophytic) and Heath species following drought-induced wildfire. 2) Mortality will continue beyond initial fire damage, indicating delayed effects and specifically, an increase in mortality risk in years five through eight. 3) Increased xeric conditions from solar radiation exposure and topographic position modify wildfire effects on cumulative delayed forest overstory mortality, with higher probability of mortality expected on xeric sites.

METHODS

Study Area Selection

The Rock Mountain Wildfire (10,208 ha), one of over a dozen large wildfires of the 2016 Southern Appalachian wildfire events, was selected as the study area (Fig. 1.1; Reilly et al., 2022). This wildfire was located within a moderate topographic position index, low-moderate burn severity (dNBR) (Reilly et al., 2022b), and has characteristic plant communities of low-mid elevation ranges in the Southern Appalachians such as forests and woodlands including northern hardwood forests, montane oak forests, cove forests, low-to-mid-elevation oak forests, pine-oak woodlands, and serpentine barrens and woodlands. Upland open communities such as high elevation outcrops, low-to mid-elevation acidic cliffs and outcrops, and low to mid elevation mafic domes, glades, and barrens are found in this region. The region incorporates wetlands such as mountain bogs, seepage wetlands, spray cliffs, bottomlands and floodplains (Edwards et al., 2013).

The study site is located within the EPA Level III Ecoregion 66, The Blue Ridge (Griffith et al. 2001). Soils range in type but are primarily comprised of sandy loams and stony loams where parent material is colluvium, or residuum weathered from granite and gneiss and/or residuum weathered from schist (USDA, 2025). The site has an 80% Inceptisol and 20% Ultisol composition (USDA, 2024) Elevation ranges from 640 meters to 1,031 meters above sea level (USGS, 2025), and the current climate is classified as a humid subtropical (Beck et al., 2018) and Towns and Rabun counties have annual rainfall

averages at 168 cm, with a minimum of 94 cm in 1986 in Towns Co, and 244 cm in 2005 in Rabun Co (Gaffin & Hotz, 2000; NOAA, 2025).

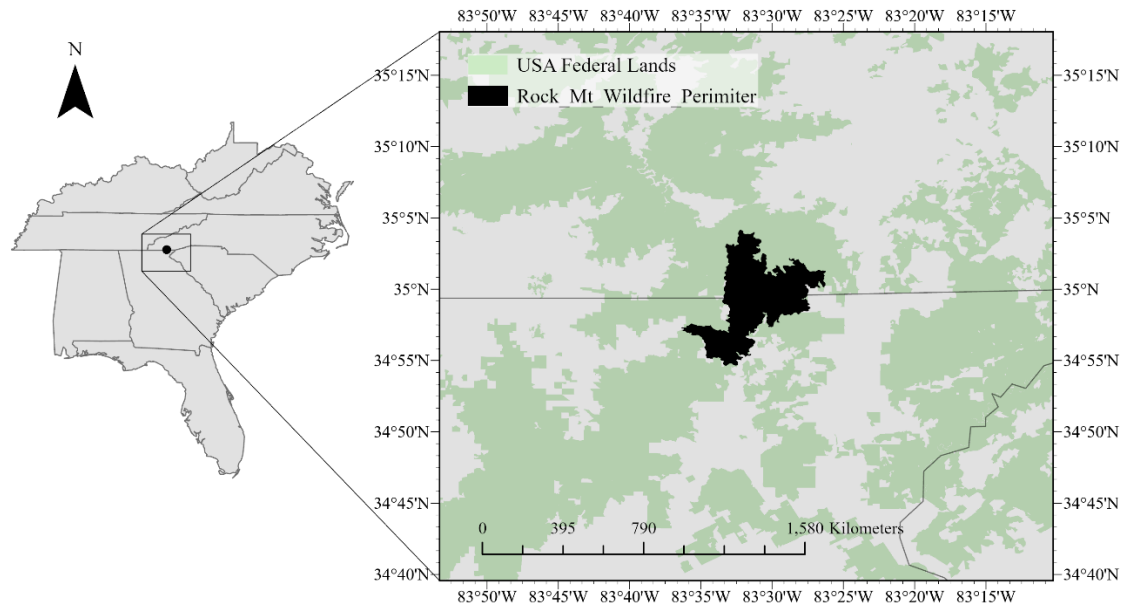


Fig. 1.1. Study area map showing the Rock Mountain Wildfire perimeter (black) in Chattahoochee National Forest, Georgia & Nantahala National Forest, North Carolina, USA. Federal Lands are denoted in green.

Group Classification

Forest overstory tree species were classified into groups by fire response criteria: bark thickness, shade tolerance, and resprouting and growth speed (Nowacki & Abrams 2008; Varner et al. 2016; Pausas 2015). Species were assigned into groups as 1) Pyrophyte with thick bark, fire-adapted resprouting ability (Arthur et al 2012; Keyser 2019; Varner et al 2016; Elliott et al. 1999), 2) Pyrophobe with thin bark and fast resprouting ability (Arthur et al 2012; Keyser 2019; Varner et al 2016), and 3) Heath, which is consistently classified

as mesophytic in literature, however has fire-adapted characteristics such as thick mature bark and resprouting ability (Elliott et al., 1999).

Three functional groups were created for the sample population: Pyrophytic (n=96) comprised of Oaks (*Quercus spp*) and Hickory (*Carya spp*), 2) Pyrophobic (n=52) comprised of Maples (*Acer spp*) and Tulip-Poplar (*Liriodendron tulipifera*), and 3) Heath (n=88) comprised of Sourwood (*Oxydendrum arbroeum*).

Study Design

In 2017, the year following wildfire, 90 permanent plots were installed across the treatment area (n=45 burned, n=45 unburned) and were distributed to capture the full range of topographic variability across the study site. Plots were square 10 x 10-m observational units (Fig. 1.2), with a total of 236 trees sampled that qualified at diameter at breast height (DBH) equal to or greater than 10.0 cm in 2017.

Annual mortality was measured during plot surveys in 2017, 2018, 2019, 2021, and 2024. DBH, mortality status, and species were determined for each qualifying tree in the plot. For each plot GPS coordinates were recorded. To examine temporal differences in mortality, measurements were grouped into an early period (1–3 years post-fire; 2017–2019) and a late period (5–8 years post-fire; 2021–2024).

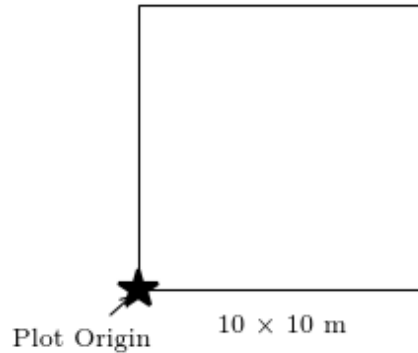


Fig. 1.2. Plot diagram of second hierarchy used in data collection at Rock Mountain Wildfire. First hierarchy level trees assigned as lowest level observational unit for forest overstory mortality data collection methods at Rock Mountain Wildfire site in Chattahoochee National Forest, Georgia, USA. Data collected in 2017, 2018, 2019, 2020, 2021, and 2024.

Variables Measured

Heat Load Index (HLI) was calculated (McCune, 2007; McCune and Keon, 2002) to quantify potential moisture stress and topographic setting. The HLI incorporates slope, aspect, and latitude for estimating incident solar radiation into a single, unitless score, ranging from 0.37 to 1.5 across the study area, with higher values indicating hotter, drier sites and lower values indicating cooler, mesic sites. Heat Load Index was calculated using the following equation:

$$HLI = \exp(-1.467 + 1.582 \cdot \cos(\lambda) \cdot \cos(\theta) - 1.500 \cdot \cos(A) \cdot \sin(\theta) \cdot \sin(\lambda) - 0.262 \cdot \sin(\lambda) \cdot \sin(\theta) + 0.607 \cdot \sin(A) \cdot \sin(\theta))$$

Where: HLI is the Heat Load Index; λ (L) is latitude in radians; θ (S) is slope in radians; and A is the folded aspect in radians, calculated as:

$$A = |\pi - |\alpha - (5\pi/4)|| = |\pi - |\alpha - 225^\circ||$$

Where: A is the folded aspect in radians; and α is the raw aspect in degrees measured clockwise from north (0–360°).

In the geographic information system (GIS) software, ArcGIS Pro v. 3.4, heat load index was calculated using a 2-meter DEM (USGS) using tools Slope (Spatial Analyst), Aspect (Spatial Analyst), and Raster Calculator. The outputs were categorized and symbolized using the Jenks Natural Breaks Method (Jenks, 1967) with five classes, and a gradient from 0.319 (blue, coldest) to 1.5 (red, warmest) (Fig. 1.3). Values were extrapolated per plot.

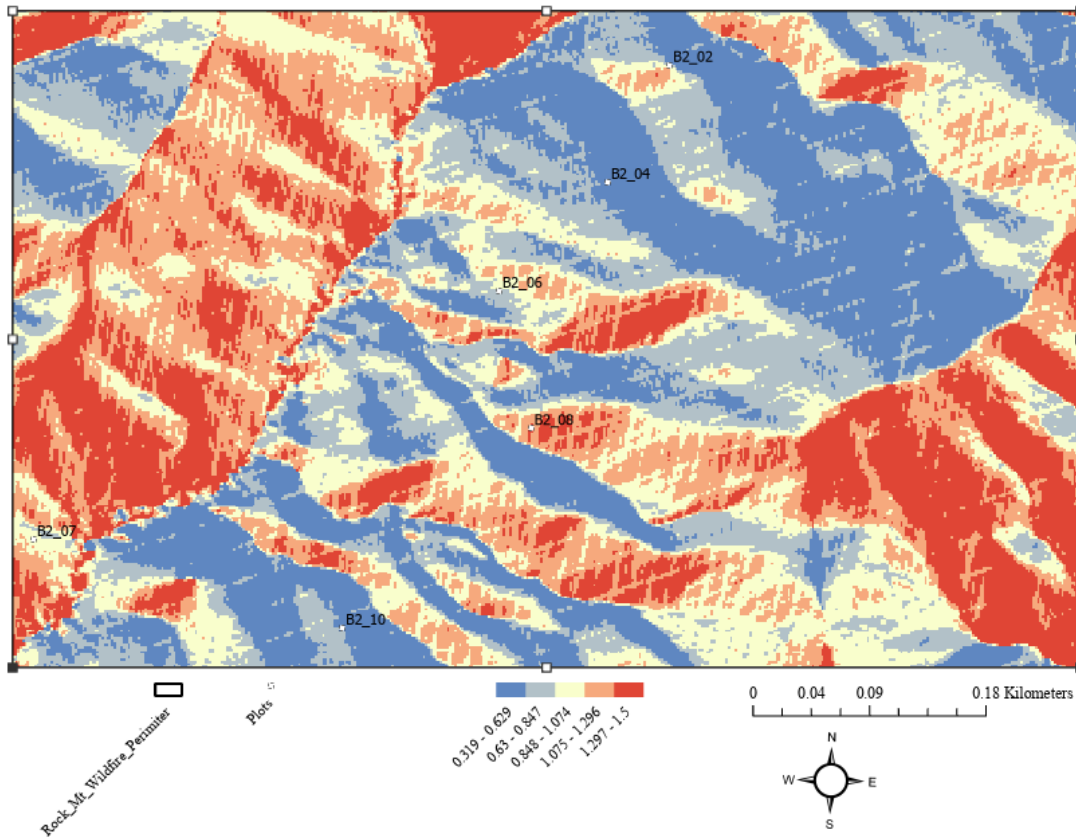


Fig. 1.3. Heat Load Index (HLI), an index that displays diffuse and direct solar radiation on site in conjunction with slope, aspect, and elevation, fixed per hemisphere (McCune & Keon 2002). HLI on site was calculated and subsequently symbolized by the Natural Breaks (Jenks) method. Displayed are a subset of plots at the study site where HLI values were extrapolated for use as a covariate. Cooler topography denoted by blue, moderate by white, and warmer, drier, xeric by red.

In-situ, qualifying overstory trees within plots were given an aluminum tag with a unique identification number in 2017 for tracking over time. Each overstory tree in the 10x10 plot greater than or equal to 10.0 cm in diameter at DBH was measured. Overstory

data were collected in 2017, 2018, 2019, 2021, and 2024 for species, mortality status, and diameter (NEON 2021; Peet et al. 1998).

Statistical Analysis

Bayesian Hierarchical Logistic Regression was chosen due to its ability to adequately handle nested sampling design of trees within plots, its hierarchical structure is suited towards direct probability statements for ecological questioning, and handling of small sample sizes using informative priors (Gelman & Hill 2007; Kéry & Royle 2016; Clark 2005).

Analysis was implemented independently using statistical languages R and JAGS (Plummer 2003) in the software RStudio 2025.09.2 Build 418 (R Core Team 2025). Three models were fitted using R package jagsUI (Kellner 2021); Data manipulation utilized tidy (Wickham et al. 2024) and dplyr (Wickham et al. 2023); visualizations were created with ggplot2 (Wickham 2016), corrplot (Wei & Simko 2021), gridExtra (Auguie 2017), and forestplot (Gordon & Lumley 2025); Multicollinearity diagnostics were performed using car (Fox & Weisberg 2019), and data were imported with openxlsx (Schauberger & Walker 2025). Statistical figures were assisted using Claude (Anthropic, 2026), a large language model.

Priors

Fixed effects across models 1, 2, and 3 used weakly informative Normal ($\mu = 0$, $\tau = 0.16$) priors, where μ is the mean and τ is precision ($\tau = 1/\sigma^2$), as is recommended for logistic regression models and reflects prior beliefs about overstory survival post-wildfire as well as to account for smaller sample sizes (Vaughn et al. 2008; Hood et al. 2018). Model 2 used weakly informative priors except for the which used an informative Normal ($\mu = -3$, $\tau = 0.16$) prior reflecting expected lower baseline hazard rates per discrete time interval of approximately five percent over three years, consistent with reported annual background mortality rates in temperate deciduous forests (Lorimer et al. 2001; Wyckoff & Clark 2002; Gonzalez-Akre et al. 2016). Plot-level random effect precision parameters used vague Gamma(0.001, 0.001) priors across all models (Kéry & Royle 2016). A correlation matrix was run to determine multicollinearity using the R package *stats* (v. 4.4.2). Specific prior assignments for each fixed effect are listed below each model equation.

Markov Chain Monte Carlo

All models were run in JAGS using Markov chain Monte Carlo (MCMC) methods. Models 2 and 3 used three chains ($nc = 3$) of 500,000 iterations ($ni = 500,000$), with a burn-in of 50,000 iterations ($nb = 50,000$) and thinning rate of 40 ($nt = 40$), yielding 33,750 posterior samples for inference. Model 1 underwent quasi-complete separation in the pyrophobe \times unburned cell, necessitating extended sampling to achieve adequate chain mixing; we therefore used $ni = 2,000,000$, $nb = 200,000$, and $nt = 80$, retaining 67,500 posterior samples (Gelman et al. 1992; Vehtari et al. 2013).

Model Fitting and Diagnostic Checks

Model fit was assessed using visual posterior predictive checks. For MCMC approximation of posterior distributions, the Gelman-Rubin statistic was used to confirm high confidence of convergence ($\hat{R} < 1.1$; Gelman & Rubin 1992; Brooks & Gelman 1998) and effective sample sizes exceeding 10,000 for key parameters. Convergence was also assessed using visual inspection of MCMC iteration traceplots. Statistical inference was made using 95% credible intervals extracted from posterior distributions and posterior probabilities for each hypothesis test.

Model Specifications

Model 1: Functional Group Response

To test differential fire sensitivity among functional groups, a logistic regression with a group \times treatment interaction was fit (Gelman & Hill, 2007).

Tree (Observational Unit)

$$\begin{aligned} \text{logit}(p_{ijk}) = & \beta_0 + \beta_{\text{trt}} \times \text{Trt}_{ij} + \beta_{\text{group}(k)} \times \text{Group}_{ijk} \\ & + \beta_{\text{trtxgroup}(k)} \times \text{Trt}_{ij} \times \text{Group}_{ijk} + \beta_{\text{dia}} \times \text{Diameter}_{ijk} + u_j \end{aligned}$$

Plot (Hierarchical Unit)

$$u_j \sim \text{Normal}(0, \sigma^2_{\text{plot}})$$

p_{ijk} = probability of mortality for tree i in plot j of group k ; Trt_{ij} = treatment (0 = unburned, 1 = burned); $Group_{ijk}$ = functional group ($k = 1$: pyrophytic reference, 2: pyrophobic, 3: heath); $\beta_{\text{group}(1)} = 0$ (reference category), u_j = random plot effect, σ^2_{plot} = between-plot variance. Priors: fixed effects (β_0 , β_{trt} , $\beta_{\text{group}(k)}$ ($k = 2$: pyrophobic, 3: heath), $\beta_{\text{trtxgroup}(k)}$ ($k = 1$: pyrophytic, 2: pyrophobic, 3: heath), $\beta_{\text{dia}} \sim \text{Normal}(\mu = 0, \tau = 0.16)$); random effect precision $\tau_{\text{plot}} \sim \text{Gamma}(0.001, 0.001)$. Derived quantities are median odds ratios for group-specific fire effects: OR 1) Pyrophytic, OR 2) Pyrophobic, and OR 3) Heath, which are determined by the following equation:

$$OR_k = \exp(\beta_{\text{trt}} + \beta_{\text{trt} \times \text{group}(k)})$$

Where OR = odds ratio, k indexes functional group, and trt = treatment (burned or unburned).

Model 2: Temporal Dynamics

Discrete-time survival analysis (Singer & Willett 1993) was implemented to compare two discrete time periods of delayed overstory mortality patterns for all species (Austin et al. 2018; Adebayo & Fahrmeir 2005). Two periods were compared 1) early (1-3 years post-wildfire, 2017-2019), and 2) late (5-8 years post-wildfire, 2021-2024), for all trees in groups.

Level 1 (Tree – period):

$$\begin{aligned} \text{logit}(h_{ijt}) = & \beta_0 + \beta_{trt} \times Trt_{ij} + \beta_{period} \times Period_t \\ & + \beta_{trt \times period} \times Trt_{ij} \times Period_t + \beta_{dia} \times Diameter_{ij} + u_j \end{aligned}$$

Level 2 (Plot):

$$u_j \sim \text{Normal}(0, \sigma^2_{plot})$$

Where h_{ijt} = hazard (conditional probability) of mortality in period t. $Period_t$ = time period (0 = early (1-3 years), 1 = late (5-8 years)). Trees dying in early period were removed from late period risk set, and other notation as in Model 1 notation above. Derived quantities were a probability of delayed overstory mortality per period via hazard risk denoted by $P(\text{delayed}) = P(\beta_{trt \times period} > 0)$, Where P is the probability fire effect increases over time.

Model 3: Solar Radiation Exposure Based on Topography

To assess topographic and solar radiation effects of wildfire to delayed overstory mortality, we assessed the Fire \times HLI interaction, to determine if delayed overstory mortality is influenced by solar radiation and topography.

Level 1 (Individual tree):

$$\begin{aligned} \text{logit}(p_{ij}) = & \beta_0 + \beta_{\text{trt}} \times \text{Trt}_{ij} + \beta_{\text{hli}} \times \text{HLI}_j + \beta_{\text{trt} \times \text{hli}} \times \text{Trt}_{ij} \times \text{HLI}_j \\ & + \beta_{\text{dia}} \times \text{Diameter}_{ij} + u_j \end{aligned}$$

Level 2 (Plot):

$$u_j \sim \text{Normal}(0, \sigma_{\text{plot}}^2)$$

HLI_j = standardized Heat Load Index for plot j , $\beta_{\text{trt} \times \text{hli}}$ = fire \times topography interaction (xeric increases mortality), and other notation as denoted above. The linear predictor included fixed effects for treatment (β_{trt}), HLI (β_{hli}), their interaction ($\beta_{\text{trt} \times \text{hli}}$), and tree diameter (β_{diameter}), with plot-level random effects ($\text{plot}_{\text{eff}(k)}$) accounting for non-independence of trees within plots. Plot random effects were drawn from a normal distribution with mean zero and estimated precision (τ_{plot}), with τ_{plot} assigned a vague Gamma(0.001, 0.001) prior. All fixed-effect priors were normal with mean zero and precision 0.16 (SD 2.5 on a logit scale), which are weakly informative (Gelman et al., 2008).

For derived quantities, predicted mortality probabilities were calculated for burned and unburned trees at $\text{HLI} = -1, 0, \text{ and } +1 \text{ SD}$, with diameter fixed at its standardized mean of zero. The posterior probability that xeric conditions amplify the fire effect was computed using the `step()` function. Posterior predictive checks were conducted by generating replicated observations (y_{rept}) from the fitted model to assess goodness of fit. Predictions

were generated using the posterior distributions of model parameters to integrate into predicted values for interpretation (Kery 2010; Makowski et al 2019), where:

$$P(xeric) = P(\beta_{trt \times hli} > 0)$$

RESULTS

Overall Delayed Forest Overstory Mortality Patterns

A total of 236 trees across burned and unburned plots at the Rock Mountain Wildfire site were included in the analysis, distributed across three functional groups: pyrophytes ($n = 96$), pyrophobes ($n = 52$), and heath species ($n = 88$; Table 1.1). Burned trees total 115 and unburned 121. Observed mortality varied by group and treatment. Among pyrophytes, mortality was 26.3% in burned and 15.5% in unburned trees. Pyrophobe mortality was 51.6% in burned trees, and 0% in unburned trees representing the quasi-complete separation condition addressed in Model 1. Heath species mortality was 47.8% in burned trees (Table 1.1). Multicollinearity among continuous covariates was low; diameter and Heat Load Index were uncorrelated ($r = 0.02$), and all models achieved convergence with $\hat{R} < 1.02$.

Table 1.1. Mortality descriptive statistics by group and treatment at rock mountain wildfire site in Chattahoochee National Forest, Georgia, USA.

Group	Treatment	Trees (<i>n</i>)	Plots (<i>n</i>)	Deaths (<i>n</i>)	Survived (<i>n</i>)
Pyrophytic					
	Burned	38	26	10	28
	Unburned	58	27	9	49
Pyrophobic					
	Burned	31	18	16	15
	Unburned	21	17	0	21
Heath					
	Burned	46	24	22	24
	Unburned	42	24	39	18

Sensitivity Analysis

Pyrophyte odds ratios are stable to prior specification (median OR range: 2.1–2.4;). Heath odds ratios show moderate sensitivity (median OR range: 10.0–15.1, and Pyrophobe odds ratios are sensitive (median OR range: 17.6–215.4), but this may be due to quasi-complete separation.

Model 1: Does fire effect increase mortality for each group

Wildfire treatment was associated with higher mortality odds across all functional groups, with the extent of effect differing for each (Fig. 1.4; Fig. 1.5; Table A1). Pyrophobes showed the strongest fire response, with mortality odds 43 times higher in burned than unburned plots (95% CI: 6.2, 598.5), followed by heath species (OR = 12.8, 95% CI: 3.8, 57.9) and pyrophytes (OR = 2.2, 95% CI: 0.7, 7.1). Credible intervals excluded one for pyrophobes and heath, indicating significant fire effects in both groups. The pyrophyte credible interval overlapped one. Pyrophobe odds ratios showed sensitivity to prior specification (median OR range: 17.6–215.4), consistent with the quasi-complete separation in the unburned cell and the wide credible interval of the primary estimate. Pyrophyte estimates were stable across prior specifications (median OR range: 2.1–2.4).

Is Fire Effect Different Between Groups (Interaction)

Fire-induced mortality varied by functional group. Both pyrophobes and heath had lower baseline mortality than pyrophytes (pyrophobic: $\beta = -2.70$, 95% CI: $-5.20, -0.64$; heath: $\beta = -1.57$, 95% CI: $-3.13, -0.18$), consistent with observed unburned mortality rates of 0%, 7.1%, and 15.5%. The fire \times pyrophobic interaction was positive ($\beta = 2.04$, 95% CI: $-0.88, 5.10$; $pd = 0.91$), with a posterior probability of 0.997 that pyrophobes experienced greater fire-induced mortality than pyrophytes (Table A2; Fig. A1).

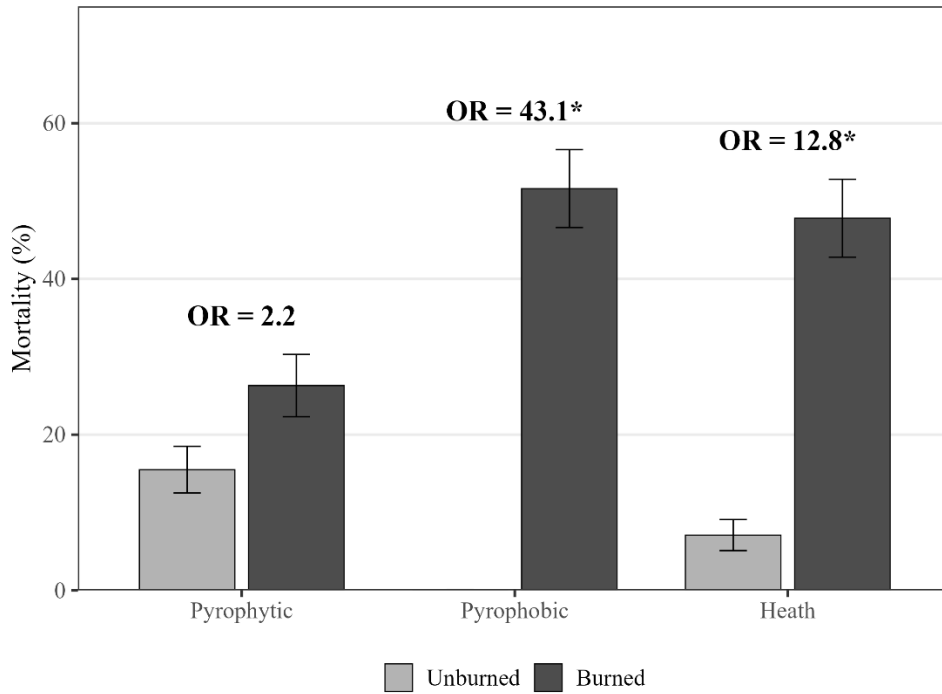


Fig. 1.4. Percent overstory mortality by functional group and fire treatment from Bayesian hierarchical logistic regression using a binomial likelihood and logit link. Analysis was based on individual tree survival status eight years post-treatment across burned and unburned plots. Light bars represent predicted mortality rates (%) in unburned control plots; dark bars represent plots burned in the 2016 Rock Mountain Fire. Error bars indicate ± 1 SE of posterior mean estimates. Median odds ratios (OR) indicate the change in mortality odds for burned versus unburned conditions within each functional group; median is reported due to posterior skewness from quasi-complete separation in the pyrophobe group. Unburned pyrophobic missing a bar due to uncertainty. Asterisks denote effects where 95% credible intervals exclude 1.0. Pyrophytic group: *Quercus montana*, *Q. coccinea*, *Q. alba*, *Q. velutina*, *Q. rubra*, *Q. falcata*; Pyrophobic group: *Acer rubrum*, *Liriodendron tulipifera*; Heath group: *Oxydendrum arboreum*.

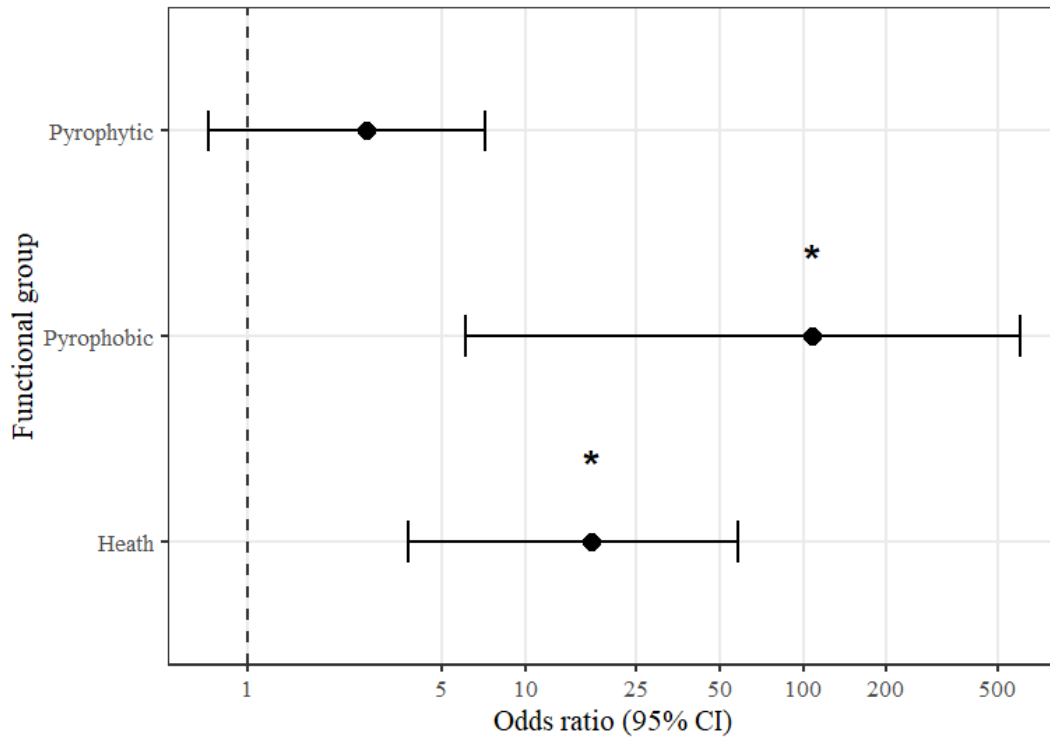


Fig. 1.5. Forest plot of fire effects on overstory mortality by group from Bayesian hierarchical logistic regression (Model 1). Points represent posterior mean estimates of fire effects on the log-odds scale; horizontal lines indicate 95% credible intervals. The vertical dashed line at one represents no effect; values to the right indicate increased mortality in burned plots relative to unburned controls. Asterisks denote effects where 95% credible intervals exclude one.

Model 2: Temporal Patterns

Fire-related mortality risk increased between the early and late post-fire periods (Table A5). Raw mortality in burned plots increased from 17.7% in the early period to 30.8% in the late period, while baseline mortality in unburned plots remained stable (Table A3). Model-predicted hazard rates in burned plots increased from 14.4% (95% CI: 7.8–22.0%) in the early period to 29.0% (95% CI: 19.1–40.1%) in the late period (Fig. 1.6; Table A4), the fire effect more than doubled between periods. The fire \times period interaction was positive ($\beta = 0.85$, 95% CI: -0.45 , 2.18 ; $pd = 0.90$), with 90% posterior probability that fire effects increased over time. Fire significantly increased mortality across both periods

($\beta = 1.36$, 95% CI: 0.41, 2.38; $pd = 1.00$), and diameter had a significant negative effect on mortality ($\beta = -0.58$, 95% CI: -1.01 , -0.19 ; $pd = 1.00$; Fig. 1.7; Table A6).

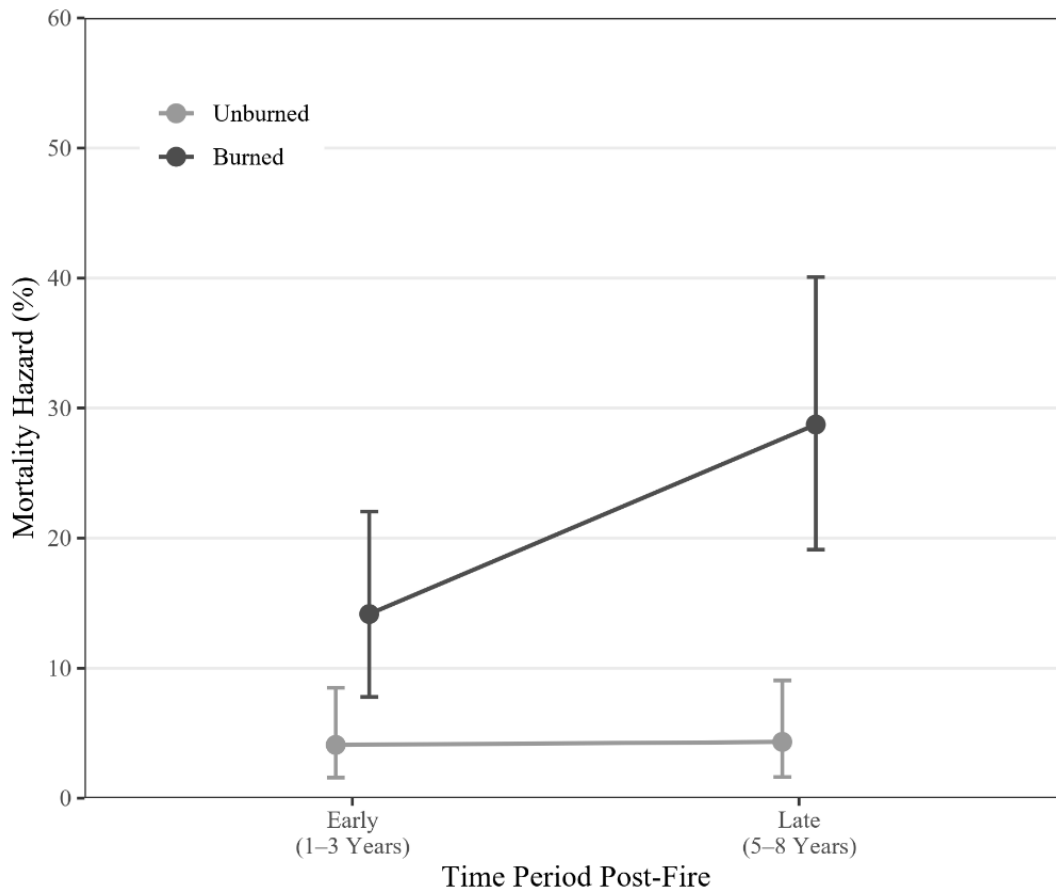


Fig. 1.6. Temporal patterns of overstory mortality hazard from Bayesian survival analysis. Points represent posterior mean hazard rates ($\pm 95\%$ credible intervals) for early (one–three years) and late (four–eight years) post-fire periods. Light symbols indicate unburned control plots, dark symbols indicate plots burned in the 2016 Rock Mountain Fire. Increasing hazard in both treatments with persistent fire effects suggests continued delayed mortality eight years post-fire. Asterisks denote significant effects.

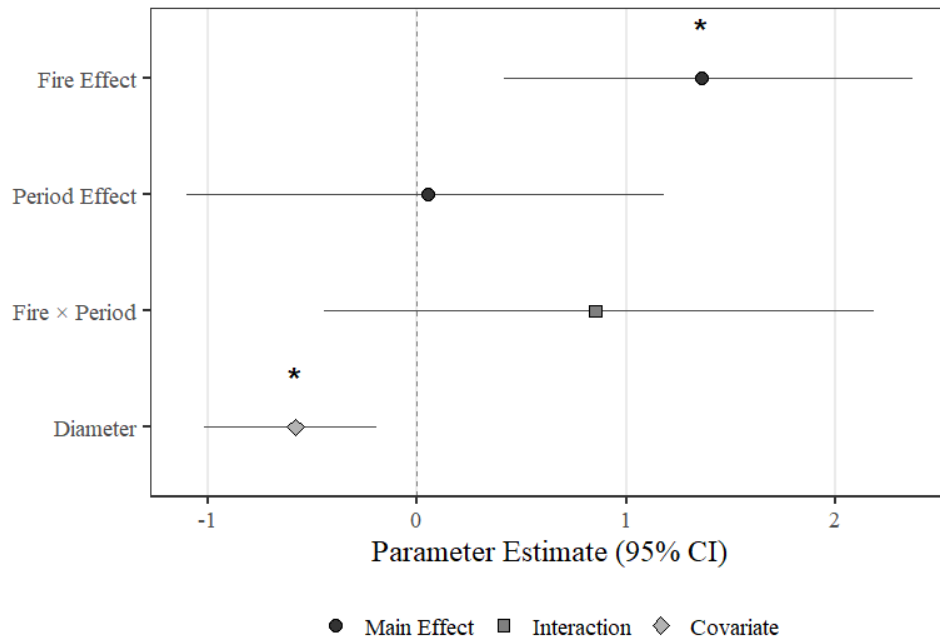


Fig. 1.7. Forest plot of key temporal pattern parameters from Bayesian hierarchical logistic regression. Points represent posterior mean estimates on log-odds scale, horizontal lines indicate 95% credible intervals. Asterisk denotes statistical significance, where credible intervals exclude 0.

Model 3: Solar Radiation Exposure Based on Topography

All models achieved convergence with \hat{R} values < 1.02 for all parameters.

Effective sample sizes exceeded 1,000 for all key parameters.

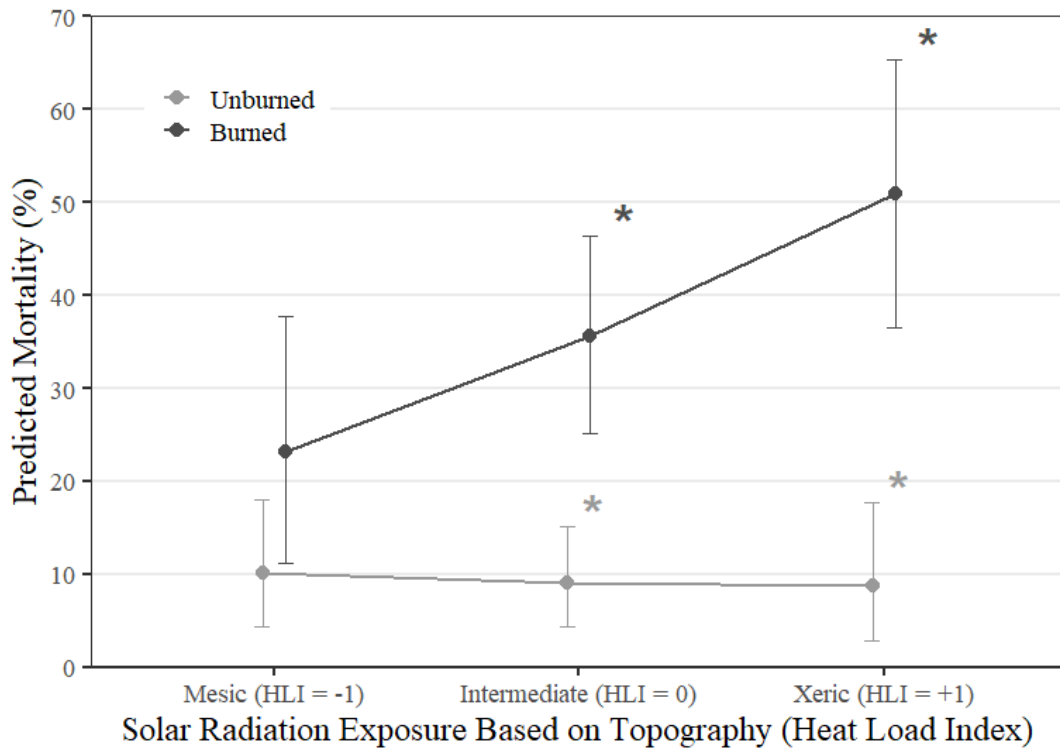


Fig. 1.8. Predicted mortality probability across the topographic Heat Load Index from Bayesian hierarchical logistic regression. Heat Load Index (HLI) represents potential solar radiation, with higher values indicating xeric southwest-facing slopes. Points show posterior mean estimates at mesic, intermediate, and xeric positions for unburned (light) and burned (dark) plots following the 2016 Rock Mountain Wildfire. Asterisks = 95% credible intervals excluding zero.

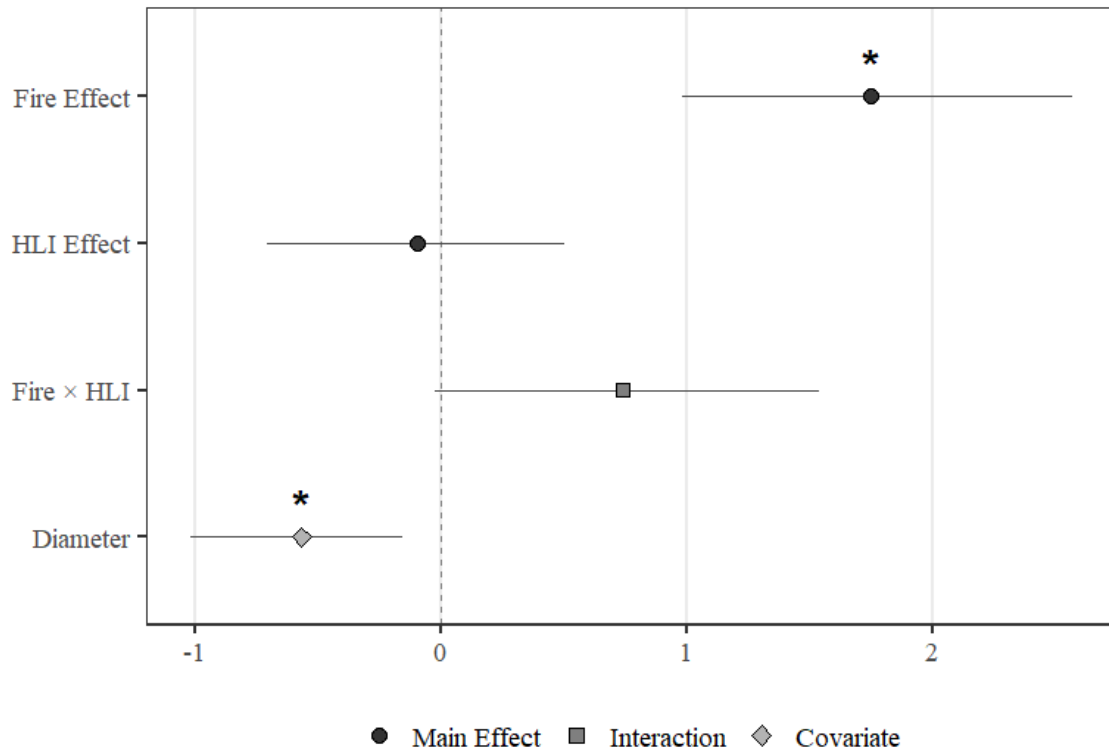


Fig. 1.9. Forest plot of key parameters from Bayesian hierarchical logistic regression, Model 3. Points represent posterior mean log-odds estimates, horizontal lines = 95% credible intervals, and the vertical line = line of no effect. Heat Load Index (HLI) represents potential solar radiation impact on soil moisture. The HLI × Fire interaction tests whether fire effects vary across solar radiation and topographic influence. Asterisks = 95% credible intervals excluding zero.

On unburned sites with low HLI index (-1), unburned mortality hazard rates are 10.1% (95% CI: 4.3–18.0%), on sites with intermediate HLI index (0), unburned mortality rates 9.1% (95% CI: 4.5–15.1%), and xeric HLI index (+1) there is unburned mortality of 8.7% (95% CI: 2.9–17.6%). On burned sites with low HLI index (-1) mortality is 23.2%

(95% CI: 11.2–37.8%), (0) = 35.6% (95% CI: 25.2–46.4%), and high index (+1) = 50.9% (95% CI: 36.5–65.5%) (Table A7, A8). There is no clear HLI effect in unburned areas, and fire effect is stronger on xeric sites. For every standard deviation increase in heat load index, there is Fire \times HLI ($\beta_{\text{fire}\times\text{HLI}} = 0.74$, $P = 0.97$). Fire effects were strongly amplified by solar radiation and topographic position (Table A7).

DISCUSSION

Fire-Intolerant (Pyrophobic) species show greater cumulative delayed forest overstory mortality than fire-adapted (Pyrophytic) and Heath species following drought-induced wildfire.

Our hypothesis is supported. Though all groups showed increased mortality odds in burned plots, the amount differed substantially: pyrophytes exhibited the smallest fire effect, followed by heath, and then pyrophobes. As noted in other studies, pyrophobes exhibit highest odds of fire sensitivity compared with fire-adapted species. Mesophytic species may be more physiologically vulnerable to the compound effects of fire and water stress; the bark is thin, exposing their vascular cambium to deadly temperatures of 60 degrees Celsius sooner than that of other species (Hood et al. 2018).

Results of this study show sourwood exhibiting intermediate fire-induced mortality. Like oaks and pines, ericaceous species concentrate fine roots in the upper 15 to 20 cm of soil of both organic soils and mineral soils (Vohník 2020), and where there is root growth in organic soils, like at Rock Mountain Wildfire, exposure to fire may make them vulnerable to the similar duff-consumption mechanisms implicated in increased pyrophyte mortality under high KBDI conditions (Carpenter et al., 2021). Although sourwood's fire-induced mortality was significant, it was still approximately three times lower than pyrophobes, suggesting partial fire tolerance. We suggest investigation into the reclassification of Heath species as an intermediate fire-response group in Southern

Appalachian fire ecology contexts, as Heath species are currently incorporated with mesophytic species.

Future research should be targeted to incorporate the combined aboveground and belowground mechanisms and drivers of these patterns. Significant Pyrophobic and Heath odds ratios in comparisons to Pyrophytic supports the hypothesis that there is greater cumulative delayed forest overstory mortality for fire-sensitive species compared with that of fire-tolerant and intermediate species after drought-induced wildfire in long unburned forests of the southern Appalachians.

**Mortality Continues Beyond Initial Fire Damage, Indicating Delayed Effects.
There Are Differences in Early-Stage Mortality (2017-2019) and Later-Stage
Mortality (2021-2024), Where There is Increased Mortality Risk in Years Five
Through Eight**

Model-predicted hazard rates for burned for plots increased from 14 percent during the 1-3 years post-fire to 29 percent 5-8 years post-fire, suggesting drivers of mortality accumulate over time for all species groupings. Fire effects suggest intensification over time for all species ($P = 0.89$), indicating mortality continues and even increases 5-8 years post-fire. This is the first documentation in Southern Appalachian hardwoods to suggest later-stage mortality.

High duff consumption from smoldering combustion that eliminated fine roots from this fire event (Carpenter et al., 2021), combined with increased late-period mortality

effects from this study may point towards physiological deterioration of trees compounding over time (O'Brien et al. 2010; Kavanagh et al. 2010; Varner et al. 2009). A cascade of physiological stress may explain why fire-induced mortality intensified from early to late period post-fire, as weakened trees were stressed enough from multiple stressors including drought and pathogens (Robbins et al. 2022).

Delayed mortality has landscape-scale implications when considering wildfire in a fire-suppressed, fire-adapted landscape undergoing global climate change. An increased mortality hazard rate in later years has implications for fire managers, who may not be able to immediately assess fire impacts to forest overstory conditions, but who do want open woodland conditions. Additionally, there are implications for post-fire fuel accumulation, with potential implications for future prescribed fire or wildfire impacts. Future research could focus on group-specific temporal differences across time periods post-fire, as well as mechanistic drivers linking belowground and aboveground effects to mortality.

Increased Xeric Conditions From Solar Radiation Exposure and Topographic Position Modify Wildfire Effects on Cumulative Delayed Forest Overstory Mortality, With Higher Probability of Mortality Expected on Xeric Sites.

Cumulative mortality over eight years shows that fire-induced mortality odds increase approximately four times from mesic sites (10%) to xeric sites (42%), with 98% posterior probability supporting interaction ($\beta_{\text{fire} \times \text{HLI}} = 0.84$). This large increase in probability likely reflects compound effects of the 2016 drought conditions and fire effects

on belowground processes and mechanisms. High KBDI values during the wildfire event promoted smoldering combustion and duff consumption (Carpenter et al. 2021). In fire-excluded southern Appalachian forests, AM and ECM fine roots colonize accumulated organic horizon (Wurzburger & Hendrick 2009), making them vulnerable to consumption during duff-consuming fires (Carpenter et al. 2021). On xeric, southwest-facing slopes, higher solar radiation increases soil temperatures by up to five degrees Celsius compared to northeast-facing slopes (McCune & Keon 2002; Seyfried et al. 2021), potentially intensifying belowground heat damage during smoldering combustion, as was seen at Rock Mountain Wildfire (Carpenter et al. 2021) (Vander Yacht et al., 2019). The resulting fine root loss initiates a decline spiral, where limited water uptake negatively influences photosynthetic capacity and the ability to repair fire damage, progressively over time (O'Brien et al. 2010). Additionally, these results are consistent with broader evidence that pre-fire drought amplifies post-fire mortality through impaired physiological function and increased fuel consumption (Cansler et al. 2024).

As climate change increases the frequency and intensity of drought periods in the Southeast, wildfire seasons will likely coincide with elevated KBDI values, increasing drought-induced fire effects on topographic positions where moisture limitation is already occurring (Williams et al. 2013; Kupfer et al. 2020). These high severity, drought-induced fires have implications for land managers who conduct prescribed fire operations in the southeast.

Limitations

Pyrophobic trees in the unburned plot predictors were almost perfect indicators of mortality: 0/21 observational units underwent mortality for the eight year timeframe. This left less variation for Model one to estimate precise effect sizes. This statistical challenge, quasi-complete separation, was addressed with informative priors. Additional limitations are that this study occurred at a single fire event. Future studies could improve Bayesian inference by expanding to multiple study sites across the southern Appalachians to increase hierarchical modeling effectiveness.

LITERATURE CITED

- Abella, S. R., Sprow, L. A., & Schetter, T. A. (2021). Delayed Tree Mortality After Prescribed Fires in Mixed Oak Forests in Northwestern Ohio. *Forest Science*, 67(4), 412–418. <https://doi.org/10.1093/forsci/xfab022>
- Adebayo, S. B., & Fahrmeir, L. (2005). Analysing child mortality in Nigeria with geoaddivitive discrete-time survival models. *Statistics in Medicine*, 24(5), 709–728.
- Anthropic. (2026). Claude (Claude Opus 4.6) Large language model. <https://claude.ai>
- Arthur, M. A., Alexander, H. D., Dey, D. C., Schweitzer, C. J., & Loftis, D. L. (2012). Refining the oak-fire hypothesis for management of oak-dominated forests of the eastern United States. *Journal of Forestry*, 110(5), 257–266. <https://doi.org/10.5849/jof.11-080>
- Auguie, B. (2017). *gridExtra: Miscellaneous functions for “Grid” graphics* (R package version 2.3). <https://CRAN.R-project.org/package=gridExtra>
- Austin, P. C., Stryhn, H., Leckie, G., & Merlo, J. (2018). A tutorial on multilevel survival analysis: Methods, models and applications. *International Statistical Review*, 86(1), 134–161.
- Beck, H. E., Zimmermann, N. E., McVicar, T. R., Vergopolan, N., Berg, A., & Wood, E. F. (2018). Present and future Köppen-Geiger climate classification maps at 1-km resolution. *Scientific Data*, 5(1), Article 180214. <https://doi.org/10.1038/sdata.2018.214>

- Brooks, S. P., & Gelman, A. (1998). General Methods for Monitoring Convergence of Iterative Simulations. *Journal of Computational and Graphical Statistics*, 7(4), 434–455. <https://doi.org/10.1080/10618600.1998.10474787>
- Cansler, C. A., Hood, S. M., Varner, J. M., van Mantgem, P. J., Agne, M. C., Andrus, R. A., Ayres, M. P., Ayres, B. D., Bakker, J. D., Battaglia, M. A., Bentz, B. J., Breece, C. R., Brown, J. K., Cluck, D. R., Coleman, T. W., Corace, R. G., Covington, W. W., Cram, D. S., Cronan, J. B., ... Wright, M. C. (2020). The Fire and Tree Mortality Database, for empirical modeling of individual tree mortality after fire. *Scientific Data*, 7(1), Article 194. <https://doi.org/10.1038/s41597-020-0522-7>
- Cansler, C. A., Wright, M. C., van Mantgem, P. J., Shearman, T. M., Varner, J. M., & Hood, S. M. (2024). Drought before fire increases tree mortality after fire. *Ecosphere (Washington, D.C)*, 15(12). <https://doi.org/10.1002/ecs2.70083>
- Carpenter, D. O., Taylor, M. K., Callahan, M. A., Jr., Hiers, J. K., Loudermilk, E. L., O'Brien, J. J., & Wurzbarger, N. (2021). Benefit or liability? The ectomycorrhizal association may undermine tree adaptations to fire after long-term fire exclusion. *Ecosystems*, 24(5), 1059–1074. <https://doi.org/10.1007/s10021-020-00568-7>
- Clark, J. S. (2005). Why environmental scientists are becoming Bayesians. *Ecology Letters*, 8(1), 2–14.
- Dey, D. C., Kabrick, J. M., & Schweitzer, C. J. (2017). Silviculture to Restore Oak Savannas and Woodlands. *Journal of Forestry*, 115(3), 202–211. <https://doi.org/10.5849/jof.15-152>

- Edwards, L., Kirkman, L. K., & Ambrose, J. (2013). *The natural communities of Georgia*.
<https://www.naturalcommunitiesofgeorgia.com/>
- Elliott, K. J., Hendrick, R. L., Major, A. E., Vose, J. M., & Swank, W. T. (1999).
Vegetation dynamics after a prescribed fire in the southern Appalachians. *Forest
Ecology and Management*, *114*(2–3), 199–213. [https://doi.org/10.1016/S0378-1127\(98\)00351-X](https://doi.org/10.1016/S0378-1127(98)00351-X)
- Flatley, W. T., Lafon, C. W., Grissino-Mayer, H. D., & LaForest, L. B. (2013). Fire history,
related to climate and land use in three southern Appalachian landscapes in the
eastern United States. *Ecological Applications*, *23*(6), 1250–1266.
<https://doi.org/10.1890/12-1752.1>
- Fox, J., & Weisberg, S. (2019). *An R companion to applied regression* (3rd ed.). Sage.
<https://socialsciences.mcmaster.ca/jfox/Books/Companion/>
- Gaffin, D. M., & Hotz, D. G. (2000). A precipitation and flood climatology with synoptic
features of heavy rainfall across the southern Appalachian Mountains. *National
Weather Digest*, *24*, 3–15.
- Gelman, A., & Rubin, D. B. (1992). Inference from Iterative Simulation Using Multiple
Sequences. *Statistical Science*, *7*(4), 457–472.
<https://doi.org/10.1214/ss/1177011136>
- Gelman, A., Jakulin, A., Pittau, M. G., & Su, Y.-S. (2008). A Weakly Informative Default
Prior Distribution for Logistic and Other Regression Models. *The Annals of Applied
Statistics*, *2*(4), 1360–1383. <https://doi.org/10.1214/08-AOAS191>

- Gonzalez-Akre, E., Meakem, V., Eng, C.-Y., Tepley, A. J., Bourg, N. A., McShea, W., Davies, S. J., & Anderson-Teixeira, K. (2016). Patterns of tree mortality in a temperate deciduous forest derived from a large forest dynamics plot. *Ecosphere*, 7(12), e01595. <https://doi.org/10.1002/ecs2.1595>
- Gordon, M., & Lumley, T. (2025). *forestplot: Advanced forest plot using 'grid' graphics* (R package version 3.1.7). <https://CRAN.R-project.org/package=forestplot>
- Griffith, G. E., Omernik, J. M., Comstock, J. A., Lawrence, S., Martin, G., Goddard, A., Hulcher, V. J., & Foster, T. (2001). *Ecoregions of Alabama and Georgia* [Map]. U.S. Geological Survey.
- Hart, J. L., Clark, S. L., Torreano, S. J., & Buchanan, M. L. (2012). Composition, structure, and dendroecology of an old-growth *Quercus* forest on the tablelands of the Cumberland Plateau, USA. *Forest Ecology and Management*, 266, 11–24. <https://doi.org/10.1016/j.foreco.2011.11.001>
- Hewson, P. (2015). *Journal of the Royal Statistical Society. Series A, Statistics in Society*, 178(1), 301–301. https://doi.org/10.1111/j.1467-985X.2014.12096_1.x
- Hood, S., & Bentz, B. (2007). Predicting postfire Douglas-fir beetle attacks and tree mortality in the northern Rocky Mountains. *Canadian Journal of Forest Research*, 37(6), 1058–1069. <https://doi.org/10.1139/X06-313>
- Hood, S. M., Varner, J. M., van Mantgem, P., & Cansler, C. A. (2018). Fire and tree death: understanding and improving modeling of fire-induced tree mortality. *Environmental Research Letters*, 13(11), 113004. <https://doi.org/10.1088/1748-9326/aae934>

- Jenks, G. F. (1967). The data model concept in statistical mapping. *International Yearbook of Cartography*, 7, 186–190.
- Kavanagh, K. L., Dickinson, M. B., & Bova, A. S. (2010). A way forward for fire-caused tree mortality prediction: Modeling a physiological consequence of fire. *Fire Ecology*, 6(1), 80–94.
- Keetch, J. J., & Byram, G. M. (1968). A drought index for forest fire control. U.S. Department of Agriculture, Forest Service, Southeastern Forest Experiment Station.
- Kellner, K. (2021). *jagsUI: A wrapper around 'rjags' to streamline 'JAGS' analyses* (R package version 1.5.2). <https://CRAN.R-project.org/package=jagsUI>
- Kéry, M. (2010). *Introduction to WinBUGS for ecologists: Bayesian approach to regression, ANOVA, mixed models and related analyses*. Academic Press.
- Kéry, M., & Royle, J. A. (2016). *Applied hierarchical modeling in ecology*. Academic Press.
- Keyser, T. L. (2019). Resprouting by seedlings of four North American deciduous broadleaved tree species following experimental burning. *Oecologia*, 190(1), 207–218. <https://doi.org/10.1007/s00442-019-04397-x>
- Kolb, T. E., Fettig, C. J., Ayres, M. P., Bentz, B. J., Hicke, J. A., Mathiasen, R., Stewart, J. E., & Weed, A. S. (2016). Observed and anticipated impacts of drought on forest insects and diseases in the United States. *Forest Ecology and Management*, 380, 321–334. <https://doi.org/10.1016/j.foreco.2016.04.051>

- Kupfer JA, Terando AJ, Gao P, Teske C, Hiers JK. (2020) Climate change projected to reduce prescribed burning opportunities in the south-eastern United States. *International Journal of Wildland Fire* 29, 764–778. <https://doi.org/10.1071/WF19198>
- Lafon, C. W., Naito, A. T., Grissino-Mayer, H. D., Horn, S. P., & Waldrop, T. A. (2017). *Fire history of the Appalachian region: A review and synthesis* (General Technical Report SRS-219). U.S. Department of Agriculture, Forest Service, Southern Research Station.
- Lorimer, C. G., Dahir, S. E., & Nordheim, E. V. (2001). Tree mortality rates and longevity in mature and old-growth hemlock-hardwood forests. *Journal of Ecology*, 89(6), 960–971. <https://doi.org/10.1111/j.1365-2745.2001.00619.x>
- Makowski, D., Ben-Shachar, M. S., & Lüdecke, D. (2019). bayestestR: Describing effects and their uncertainty, existence and significance within the Bayesian framework. *Journal of Open Source Software*, 4(40), 1541.
- Makowski, D., Ben-Shachar, M. S., Chen, S. H. A., & Lüdecke, D. (2019). Indices of effect existence and significance in the Bayesian framework. *Frontiers in Psychology*, 10, 2767. <https://doi.org/10.3389/fpsyg.2019.02767>
- McCune, B., & Keon, D. (2002). Equations for potential annual direct incident radiation and heat load. *Journal of Vegetation Science*, 13(4), 603–606. <https://doi.org/10.1111/j.1654-1103.2002.tb02087.x>

- McCune, B. (2007). Improved estimates of incident radiation and heat load using non-parametric regression against topographic variables. *Journal of Vegetation Science*, 18(5), 751–754. <https://doi.org/10.1111/j.1654-1103.2007.tb02590.x>
- NEON (National Ecological Observatory Network). (2021). *TOS Protocol and Procedure: Measurement of Vegetation Structure*. NEON.DOC.000987. Available at: <https://data.neonscience.org/>
- NOAA National Centers for Environmental Information. (2025, January). *Climate at a glance: County time series*. <https://www.ncei.noaa.gov/access/monitoring/climate-at-a-glance/county/time-series>
- Nowacki, G. J., & Abrams, M. D. (2008). The Demise of Fire and “Mesophication” of Forests in the Eastern United States. *Bioscience*, 58(2), 123–138. <https://doi.org/10.1641/B580207>
- O’Brien, J. J., Hiers, J. K., Mitchell, R. J., Varner, J. M. I., & Mordecai, K. (2010). Acute Physiological Stress and Mortality Following Fire in a Long-Unburned Longleaf Pine Ecosystem. *Fire Ecology*, 6(2), 1–12. <https://doi.org/10.4996/fireecology.0602001>
- Pausas, J. G. (2015). Bark thickness and fire regime. *Functional Ecology*, 29(3), 315–327. <https://doi.org/10.1111/1365-2435.12372>
- Peet, R. K., Wentworth, T. R., & White, P. S. (1998). A flexible, multipurpose method for recording vegetation composition and structure. *Castanea*, 63(3), 262–274.
- Plummer, M. (2003). JAGS: A program for analysis of Bayesian graphical models using Gibbs sampling. In K. Hornik, F. Leisch, & A. Zeileis (Eds.), *Proceedings of the*

- 3rd International Workshop on Distributed Statistical Computing (DSC 2003)*.
Vienna, Austria. <https://www.r-project.org/conferences/DSC-2003/Proceedings/>
- R Core Team. (2025). *R: A language and environment for statistical computing*. R Foundation for Statistical Computing. <https://www.R-project.org/>
- Reilly, M. J., Norman, S. P., O'Brien, J. J., & Loudermilk, E. L. (2022). Drivers and ecological impacts of a wildfire outbreak in the southern Appalachian Mountains after decades of fire exclusion. *Forest Ecology and Management*, 524(C), Article 120500. <https://doi.org/10.1016/j.foreco.2022.120500>
- Robbins, Z. J., Loudermilk, E. L., Mozelewski, T. G., Jones, K., & Scheller, R. M. (2024). Fire regimes of the Southern Appalachians may radically shift under climate change. *Fire Ecology*, 20(1), Article 2. <https://doi.org/10.1186/s42408-023-00231-1>
- Robbins, Z. J., Loudermilk, E. L., O'Brien, J. J., Pokswinski, S. M., Hornsby, B. S., Loudermilk, A. E., & Hiers, J. K. (2022). Delayed fire mortality has long-term ecological effects across the Southern Appalachian landscape. *Ecosphere*, 13(6), e4153. <https://doi.org/10.1002/ecs2.4153>
- Singer, J. D., & Willett, J. B. (1993). It's about time: Using discrete-time survival analysis to study duration and the timing of events. *Journal of Educational Statistics*, 18(2), 155–195. <https://doi.org/10.3102/10769986018002155>
- Seyfried, M., Flerchinger, G., Bryden, S., Link, T., Marks, D., & McNamara, J. (2021). Slope and aspect controls on soil climate: Field documentation and implications for

- large-scale simulation of critical zone processes. *Vadose Zone Journal*, 20(6).
<https://doi.org/10.1002/vzj2.20158>
- United States Department of Agriculture, Natural Resources Conservation Service. (2024).
USA soils map units (Data set). Esri ArcGIS Living Atlas.
<https://www.arcgis.com/home/item.html?id=06e5fd61bdb6453fb16534c676e1c9b9>
- United States Department of Agriculture, Natural Resources Conservation Service. (2025).
Custom soil resource report for Dawson, Lumpkin, and White Counties, Georgia; Fannin and Union Counties, Georgia; Habersham County, Georgia; and Rabun and Towns Counties, Georgia. <https://websoilsurvey.sc.egov.usda.gov/>
- U.S. Geological Survey. (2025). *Digital elevation model* (Data set). Earth Explorer.
<https://earthexplorer.usgs.gov/>
- van Mantgem, P. J., Nesmith, J. C. B., Keifer, M., Knapp, E. E., Flint, A., & Flint, L. (2013). Climatic stress increases forest fire severity across the western United States. *Ecology Letters*, 16(9), 1151–1156. <https://doi.org/10.1111/ele.12151>
- Vaughn, B. K. (2008). (Rev. of *Data analysis using regression and multilevel/hierarchical models*, by Gelman, A., & Hill, J). *Journal of Educational Measurement*, 45(1), 94–97. https://doi.org/10.1111/j.1745-3984.2007.00053_2.x
- Varner, J. M., III, Putz, F. E., O'Brien, J. J., Hiers, J. K., Mitchell, R. J., & Gordon, D. R. (2009). Post-fire tree stress and growth following smoldering duff fires. *Forest Ecology and Management*, 258(11), 2467–2474.

- Varner, J. M., Kane, J. M., Hiers, J. K., Kreye, J. K., & Veldman, J. W. (2016). Suites of Fire-Adapted traits of Oaks in the Southeastern USA: Multiple Strategies for Persistence. *Fire Ecology*, *12*(2), 48–64. <https://doi.org/10.4996/fireecology.1202048>
- Vehtari, A., Gelman, A., Carlin, J. B., Stern, H. S., Dunson, D. B., & Rubin, D. B. (2013). Part II: Fundamentals of Bayesian Data Analysis. In *Bayesian Data Analysis*. CRC Press LLC.
- Vohník, M. (2020). Ericoid mycorrhizal symbiosis: Theoretical background and methods for its comprehensive investigation. *Mycorrhiza*, *30*(6), 671–695. <https://doi.org/10.1007/s00572-020-00989-1>
- Wei, T., & Simko, V. (2021). *R package 'corrplot': Visualization of a correlation matrix* (Version 0.92). <https://github.com/taiyun/corrplot>
- Wickham, H., François, R., Henry, L., Müller, K., & Vaughan, D. (2023). *dplyr: A grammar of data manipulation* (R package version 1.1.4). <https://CRAN.R-project.org/package=dplyr>
- Wickham, H., Vaughan, D., & Girlich, M. (2024). *tidyr: Tidy messy data* (R package version 1.3.1) <https://CRAN.R-project.org/package=tidyr>
- Wickham, H. (2016). *ggplot2: Elegant graphics for data analysis* (2nd ed.). Springer-Verlag. <https://ggplot2.tidyverse.org>
- Williams, A. P., Allen, C. D., Macalady, A. K., Griffin, D., Woodhouse, C. A., Meko, D. M., Swetnam, T. W., Rauscher, S. A., Seager, R., Grissino-Mayer, H. D., Dean, J. S., Cook, E. R., Gangodagamage, C., Cai, M., & McDowell, N. G. (2013).

- Temperature as a potent driver of regional forest drought stress and tree mortality. *Nature Climate Change*, 3, 292–297. <https://doi.org/10.1038/nclimate1693>
- Wurzburger, N., & Hendrick, R. L. (2009). Plant litter chemistry and mycorrhizal roots promote a nitrogen feedback in a temperate forest. *Journal of Ecology*, 97(3), 528–536. <https://doi.org/10.1111/j.1365-2745.2009.01487.x>
- Wyckoff, P. H., & Clark, J. S. (2002). The Relationship between Growth and Mortality for Seven Co-Occurring Tree Species in the Southern Appalachian Mountains. *The Journal of Ecology*, 90(4), 604–615. <https://doi.org/10.1046/j.1365-2745.2002.00691.x>
- Yarnell, S. L., & United States. Forest Service. Southern Research Station. (1998). *The Southern Appalachians a history of the landscape*. U.S. Dept. of Agriculture, Forest Service, Southern Research Station <http://purl.access.gpo.gov/GPO/LPS59396>

CHAPTER TWO: FOREST REGENERATION PATTERNS FOLLOWING WILDFIRE IN THE SOUTHERN APPALACHIANS

INTRODUCTION

Southern Appalachian Mountain forests have been maintained by cultural and natural disturbances for centuries prior to fire exclusion and suppression policies of the early 20th century (Lafon et al. 2017; Flatley et al. 2013; McEwan et al. 2007). Where historical structure and composition of oak forests were previously fire-maintained (McEwan et al 2007), the onset of these policies influenced forest structure and composition towards a more closed-canopy forest that has led to mesophication (Hutchinson et al 2008). Over the past 30 years, prominent oak forests have seen a decline in density yet an increase in volume. Approximately 87% of the Central Hardwood Region experienced density decreases in oak, with the most occurring in the southern Appalachians and Cumberland Plateau (Fei et al. 2011).

Fire suppression and exclusion policies dynamically and directly impact fire return intervals and forest dynamics in southern Appalachian Forest, shifting the median fire return interval from approximately 5.4 years to effectively fire-free conditions over the past 80 to 100 years (Lafon et al. 2017; Arthur et al. 2021). A lack of historical fire frequency has led to shifts in understory herbaceous species, wildlife habitat, and forest structure (Harper et al 2016; Dey et al. 2017; McShea et al. 2007). Formally described by Nowacki and Abrams (2008), mesophication is the process by which formerly oak dominated forests have shifted in composition towards increasingly shade-tolerant and

fire-sensitive overstory species such as Red Maple (*Acer rubrum*) and Tulip-Poplar (*Liriodendron tulipifera*), which then promote more shade-tolerant and fire-sensitive overstory species in continuity. This dynamic is due to fire-suppression occurring in Eastern North American Forests (Woodbridge et al. 2022; Fei et al. 2011 Palus et al. 2018; Alexander & Arthur 2014), and in Europe, mesophication has already completed a forest compositional shift from fire-adapted to mesophytic species (Spînu et al. 2020). Mesophication directly threatens regeneration of fire-adapted Eastern US forest overstory species such as oaks, pines, and hickories that depend on more open-understory conditions, with shading, increased leaf litter moisture, and an increase in nutrients (Legge et al. 2025; Nowacki and Abrams, 2008).

In addition to aboveground processes, compound effects of the 2016 drought conditions had implications on belowground processes; burned high KBDI soils promoted smoldering combustion and duff consumption (Carpenter et al. 2021). Additionally, heat stress to soil is impacted by climactic inputs, as xeric, southwest-facing slopes have higher solar radiation that increase soil temperatures by up to five degrees Celsius compared to northeast-facing slopes (McCune & Keon 2002; Seyfried et al. 2021).

Removal of the organic layer after wildfire may have implications for forest regeneration patterns undergoing mesophication. In the Southern Appalachians there are documented soil horizons and mycorrhizal impacts following drought-induced wildfire

(Carpenter et al. 2020), although the implications for forest overstory regeneration remain relatively unstudied.

Research over the past two decades has demonstrated that forest regeneration patterns following prescribed fire are influenced by topographic position and soil moisture regimes. Prescribed fire effects on regeneration are impacted by topography, with oak and hickory regeneration increasing density on dry ridges and intermediate landscape positions, while fire treatments decreased density on mesic sites (Hutchinson et al. 2024). This pattern is consistent and influences land management efforts that promote oak regeneration, which suggest focus on xeric to intermediate sites (Iverson et al. 2017). In addition, forest regeneration of differing plant communities after wildfire has been studied in the Southern Appalachians, and found oaks responded positively to burning twice in thermic oak communities (Hagan et al. 2015). In contrast, Red Maple (*Acer rubrum*) and Tulip-Poplar (*Liriodendron tulipifera*) increase density in areas treated with low-intensity fire or left unburned, and may outcompete oaks on productive sites (Beasley et al., 2022; Keyser et al., 2019; Iverson et al., 2017). The objectives of the study were to assess wildfire impacts to forest regeneration in long unburned forests undergoing mesophication, and to assess if that regeneration varied by plant community and topographic position. Our hypotheses are as follows: 1: Drought-induced wildfire increases the relative abundance of pyrophyte regeneration relative to mesophytes. 2: Drought-induced wildfire effects on regeneration differ by topographic orientation, with strongest pyrophyte response in historically fire-maintained plant communities.

METHODS

Study Area Selection

The Rock Mountain Wildfire (10,208 ha) from the 2016 wildfire outbreak events in the Southern Appalachians, was selected as the study area (Reilly et al., 2022). This wildfire was located within a moderate topographic position index, low-moderate burn severity (dNBR) (Reilly et al, 2022), and has characteristic plant communities of low-mid elevation ranges in the Southern Appalachians such as forests and woodlands including northern hardwood forests, montane oak forests, cove forests, low-to-mid-elevation oak forests, pine-oak woodlands, and serpentine barrens and woodlands.

The study site is located within the EPA Level III Ecoregion 66, The Blue Ridge (Griffith et al. 2001). Soils range in type but are primarily comprised of sandy loams and stony loams where parent material is colluvium, or residuum weathered from granite and gneiss and/or residuum weathered from schist (USDA 2025). The site has an 80% Inceptisol 20% Ultisol composition (Esri, 2024). Elevation ranges from 640 meters to 1,031 meters above sea level (USGS, 2025), and the climate is classified as a humid subtropical (Beck et al. 2018) and Towns and Rabun counties have annual rainfall averages at 168 cm, with a minimum of 94 cm in 1986 in Towns Co, and 244 cm in 2005 in Rabun Co (Gaffin& Hotz, 2000; NOAA, 2025).

Experimental Design

A randomized complete block design with stratification design with a treatment level of burned and unburned (n=2), with a blocking factor of watershed (n=3) was applied. Plant communities were stratified as: 1) Bottomland/Cove, 2) Mid-slope Oak/Pine, and 3) Thermic Oak, Oak/Pine (n=3), and measurement plots were randomly assigned within. Data was collected in Fall 2024, eight years following the wildfire event.

Data Collection

In 2024, eight years post-fire treatment, 90 permanent subplots were installed across the treatment area (n=45 burned, n=45 unburned) and were distributed to capture the full range of topographic variability across the study site. Plots were square 3 x 3-m observational units (Fig. 2.1), and tree regeneration was measured for qualifying individuals. All woody tree species occurring in the plot were identified, counted, and recorded by their size class: seedlings (10-50cm, 50-100cm, & 100-137cm in height off of the forest floor) and saplings (0-1cm at DBH, 1-2.5cm at DBH) (NEON 2021; Peet et al. 1998). Plant communities were documented in accordance with The Natural Communities of Georgia for grouping into categories suitable for statistical analysis (Edwards et al., 2013).

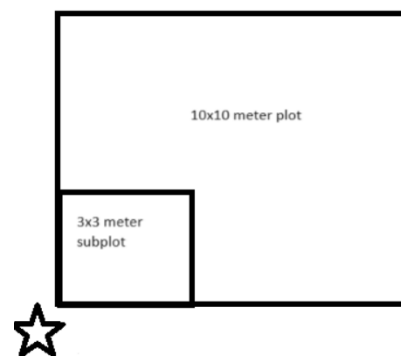


Fig. 2.1 Plot diagram of 3x3 m observational units used in data collection at Rock Mountain Wildfire site in Chattahoochee National Forest, Georgia, USA. Data collected in 2024.

Environmental Covariates

Heat Load Index (HLI) was calculated (McCune, 2007; McCune and Keon, 2002) to quantify potential moisture stress and topographic setting. HLI calculates landscape slope, landscape aspect, and latitude that estimates potential direct incident radiation, with higher values indicating hotter, drier sites and lower values indicating cooler, more mesic sites. Heat Load Index was calculated using the following equation:

$$HLI = \exp(-1.467 + 1.582 \cdot \cos(\lambda) \cdot \cos(\theta) - 1.500 \cdot \cos(\alpha) \cdot \sin(\theta) \cdot \sin(\lambda) - 0.262 \cdot \sin(\lambda) \cdot \sin(\theta) + 0.607 \cdot \sin(\alpha) \cdot \sin(\theta))$$

Where: *HLI* is Heat Load Index, λ (L) is latitude in radians, θ (S) is slope in radians, α (A) is the folded aspect (A), is in radians for the northern hemisphere:

$$A = |\pi - |\alpha - (5\pi/4)|| = |\pi - |\alpha - 225^\circ||$$

Folded aspect reorients the 0-360 scale to a zero to one scale that reflects warmer areas of southwest-facing slopes and the cooler areas of northeast-facing slopes. In the spatial software, ArcGIS Pro v. 3.4, heat load index was calculated using a 2-meter DEM (USGS, 2024) using tools Slope (Spatial Analyst), Aspect (Spatial Analyst), and Raster Calculator. The outputs were categorized with five classes and symbolized using the Jenks Natural Breaks Method, which minimizes variance within each class while

maximizing variance between classes (North 2009). The output gradient ranges from 0.319 (blue, coldest) to 1.5 (red, warmest). Values were extrapolated per plot.

Data Analysis

Multicollinearity

To test whether continuous HLI was associated with plant communities, an ANOVA with eta-squared (η^2) effect sizes, was used, and Variance of Inflation Factors (VIF) was calculated for all predictors, with $VIF > 5$ indicating concerns.

Group Classification

We classified groups by fire response of criteria: bark thickness, and resprouting and growth speed (Nowacki & Abrams 2008; Varner et al. 2016; Lorimer et al. 1994; Pausas 2015). Species were assigned into groups as 1) a Pyrophyte with thick bark, fire-adapted resprouting ability, and are Oaks (*Quercus spp*) and Hickories (*Carya spp*) (Arthur et al 2012; Keyser 2019; Varner et al 2016), and 2) Pyrophobe with thin bark and fast resprouting ability, which are Red Maple (*Acer rubrum*) and Tulip-Poplar (*Liriodendron tulipefera*) (Arthur et al 2012; Keyser 2019; Varner et al 2016). Fire-adapted Yellow Pines (*Pinus virginiana*, *P. echinata*) were excluded due to small sample sizes.

Response variables are 1) Absolute Density (stems/hectare) and is the sum of species within each group, scaled to stems/ha; and 2) Relative Abundance (group stems/

stems per plot) scaled to hectare. These response variables are bounded for beta regression from 0-1.

Non-Metric Multidimensional Scaling

Regeneration composition was analyzed using non-metric multidimensional scaling (NMDS) ordination (Kruskal 1964) to visualize community composition differences using Bray-Curtis distance metrics for relative abundance (Bray & Curtis 1957). Genus-level relative abundances were calculated from combined seedling and sapling densities, where species vectors categorized by functional groups. Ordination was evaluated by comparing stress values (Clarke 1993) and testing correlations with treatment and plant community. The NMDS analysis itself was run in software R version 4 (R Core Team 2024), vegan package (Oksanen et al. 2024). Statistical figures were created with the assistance of Claude, a large language model (Anthropic, 2026).

Wilcoxin Rank Sum Test

Pooled comparisons of group-level regeneration density between burned and unburned treatments were conducted using Wilcoxon rank-sum tests. Data were pooled across plant communities to assess overall treatment effects on pyrophyte and pyrophobe regeneration density. Wilcoxon rank-sum tests were selected due to density distributions that violated normality assumptions (Shapiro-Wilk test, $p < 0.05$).

Generalized Linear Mixed Models

Regeneration density (stems/hectare) was modeled for Pyrophytes and Pyrophobes, using generalized linear mixed models (GLMMs) with a negative binomial distribution and log link to account for overdispersion in the count data, and used the following equation:

$$\log(\mu_{ij}) = \beta_0 + \beta_1 T_i + \beta_2 C_i + \beta_3 (T \times C)_i + \beta_4 \text{HLI}_i + u_j$$

where μ_{ij} is expected density for plot i in block j , T is treatment (burned/ unburned), C is assigned plant community, HLI is a solar radiation and topographic covariate, and $u_j \sim N(0, \sigma^2)$ is a random intercept for block. Derived quantities are ratios.

Relative abundance (Per observational unit, relative abundance = Group Density / (Total Density + 0.001)) was modeled for Pyrophytes and Pyrophobs using beta regression GLMMs, logit link:

$$\text{logit}(\mu_{ij}) = \beta_0 + \beta_1 T_i + \beta_2 C_i + \beta_3 (T \times C)_i + \beta_4 \text{HLI}_i + u_j$$

Proportions were bounded away from zero and one using a squeeze transformation. HLI was centered and scaled. Derived quantities are odds ratios.

Model Fitting

Separate models were fit for each species group: Pyrophyte and Pyrophobe. Density models used a negative binomial distribution. Zero-inflation was evaluated but not included in final models, where $zifformula = 0$ (Bolker et al. 2009; Zuur et al. 2009).

Relative abundance models used beta regression (Douma & Weedon 2019). All models were fit using the glmmTMB package (Brooks et al. 2017) in R 2025.09.2+418 (R Core Team 2024), and zero-inflation was not needed for Pyrophyte or Pyrophobe. Model convergence was verified by checking for standard errors. Model fit was assessed using DHARMA residual diagnostics (Hartig 2022), as DHARMA diagnostics indicated no significant overdispersion or zero-inflation for Pyrophytes and Pyrophobes ($p > 0.05$; ZI less than 11 percent). Statistical figures were assisted using Claude (Anthropic, 2026), a large language model.

Inference

Statistical significance of fixed effects was assessed using Type III Wald chi-square tests (Fox & Weisberg 2019). Post-hoc pairwise contrasts were conducted using estimated marginal means (Lenth 2024) to compare treatments to both overall, averaged across plant communities, as well as within each plant community. Derived quantities for density models where treatment effects are reported as ratios of estimated means. For relative abundance models, treatment effects are reported as odds ratios, using a significance threshold of $\alpha = 0.05$. Multiple comparisons were adjusted using the false discovery rate method (FDR) (Benjamini & Hochberg 1995). Analyses were conducted in R using glmmTMB (Brooks et al 2017) for model fitting, and emmeans for contrasts (Lenth 2024).

RESULTS

Multicollinearity

Collinearity diagnostics indicated moderate correlation between HLI and low ($r = 0.14$), and plant communities showed moderate association with HLI ($\eta^2 = 0.13$, $p = 0.007$), and all VIF values were < 5 . HLI and plant community groupings were kept, as plant communities represent broad vegetation assemblages, while HLI captures topographic heterogeneity due to abiotic influences such as solar radiation, slope, and aspect, capturing different biological systems.

Non-Parametric Analysis

Non-Metric Multidimensional Scaling

NMDS observed dissimilarity for absolute density show a linear fit of 0.904 and a non-metric fit = 0.971 (Fig. 2.2). The ordination plot (Fig. 2.3), shows relative distances between observational units (plots), indicating patterns which are detailed below.

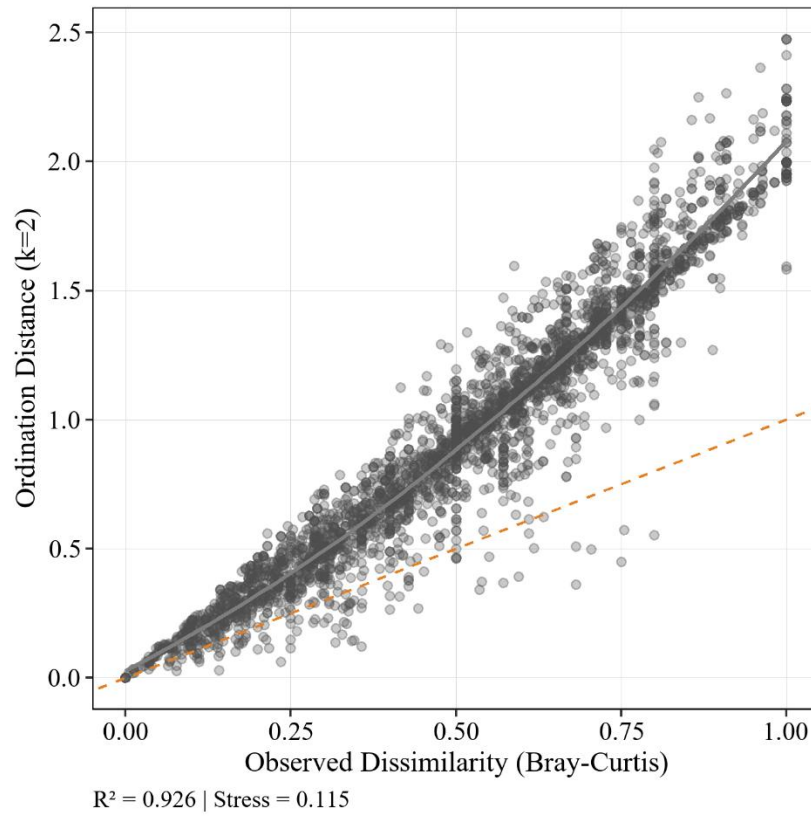


Fig. 2.2 Shepard plot for two-dimensional ($k=2$) non-metric multidimensional scaling ordination showing observed Bray-Curtis dissimilarities versus ordination distances. Stepped line represents the non-metric fit and the dashed line represents linear fit.

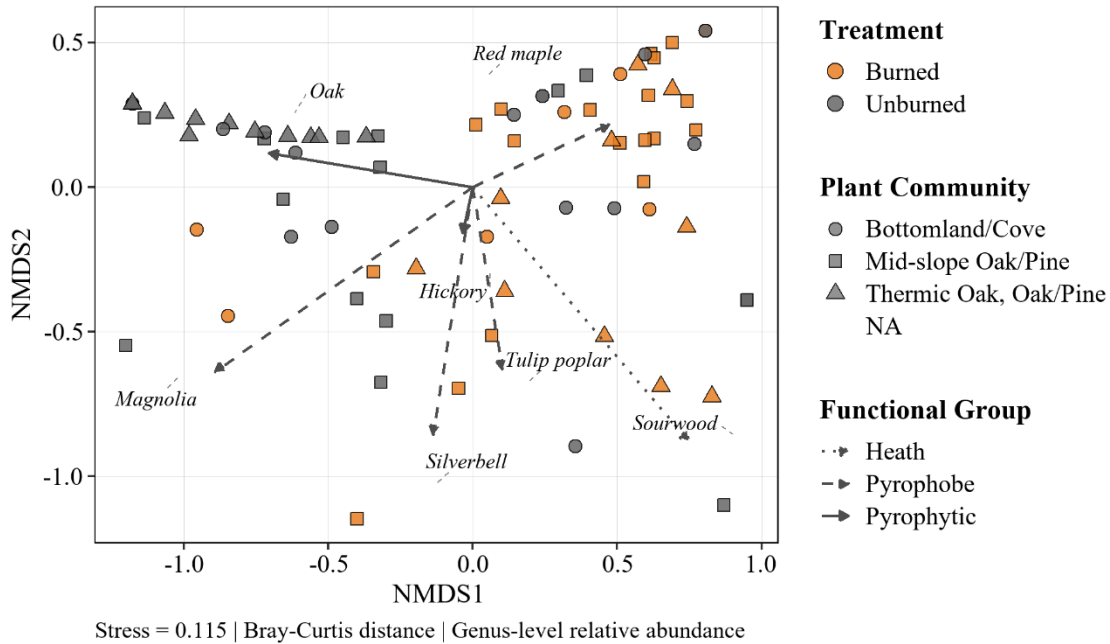


Fig. 2.3. Results of non-metric multidimensional scaling ordination of overstory trees at Rock Mountain using a Bray-Curtis dissimilarity distance measure. Analysis was based on genus-level relative abundance in each plot. Gray symbols are unburned plots and orange symbols are burned plots. Circles represent Bottomland/Cove communities, squares represent Mid-slope Oak/Pine communities, and triangles represent Thermic Oak/Oak-Pine communities. Arrows represent species vectors showing direction and magnitude of increasing abundance: solid arrows indicate pyrophytic species, dashed arrows indicate pyrophobic species, and dotted arrows indicate heath species. Final stress for the two-dimensional solution was 0.115.

Overall NMDS Patterns

Burned and unburned plots separated in NMDS ordination space (2D, stress = 0.115; Fig. 2.3). Species vectors show a pyrophyte to mesophyte gradient, with burned plots going toward pyrophytic dominance and unburned plots toward mesophytes. Sourwood (*Oxidendron arboreum*) appeared in fewer than a quarter of plots and did not drive community separation (Fig. 2.3.)

NMDS Species Relative Abundance Regeneration Patterns:

Burned and unburned areas are separated in ordination space, showing a distinct pattern difference in oak regeneration for unburned areas in most communities but dominated by mid-slope and thermic communities. Red Maple shows a distinct difference in proportions for all plant communities of the burned treatment. Sourwood shows a distinct pattern towards burned thermic oak communities and unburned midslope. These differences were most pronounced in drier plant communities. Heat Load Index and Topographic Moisture Index, were not confounded by topographic position, and are not significant predictors of regeneration density and relative abundance (stems/ha) for combined species groups ($P > 0.10$; Fig. 2.3.)

Wilcoxin Rank Sum Test

Burned plots have approximately twice the amount of raw regeneration density than unburned plots, with 38,832 stems/ha compared to 19,709 stems/ha. In unburned plots, pyrophyte regeneration was most abundant (13,685 stems/ha), followed by pyrophobe regeneration (6,179 stems/ha). In burned plots, pyrophobe density was most abundant at 30,794 stems/ha and statistically significantly higher, while pyrophyte regeneration density was 5,905 stems/ha (Table 2.1).

Table 2.1. Regeneration density (stems/ha \pm SE) by species group and treatment at rock mountain wildfire study site.

Species Group	Unburned	Burned	W	p
Pyrophyte	13,685 \pm 3,728	5,905 \pm 884	621.5	0.318
Pyrophobe	6,179 \pm 1,270	30,794 \pm 6,498 ***	1,224.5	<0.001

Generalized Linear Mixed-Effects Model - Chi-Square Inference

Type III Wald chi-square tests revealed no significant main effect of wildfire on regeneration density for any functional group for all communities (all $p > 0.05$; Table B1). Pyrophobes showed a marginal response to fire ($\chi^2 = 3.95$, $df = 1$, $p = 0.05$), whereas Pyrophytes did not ($\chi^2 = 0.31$, $df = 1$, $p = 0.58$). None of the treatment \times plant community interactions reached significance for density ($p > 0.45$). For relative abundance, the treatment \times plant community interaction was significant for Pyrophytes ($\chi^2 = 8.88$, $df = 2$,

$p = 0.01$), indicating that wildfire effects on species composition depend on plant community type (Table B2). Pyrophobes showed no interaction ($\chi^2 = 2.76$, $df = 2$, $p = 0.25$). Heat load index strongly predicted relative abundance for both Pyrophytes ($\chi^2 = 25.88$, $df = 1$, $p < 0.001$) and Pyrophobes ($\chi^2 = 12.72$, $df = 1$, $p < 0.001$), though it had no effect on absolute density. Post-hoc contrasts examining treatment effects within each plant community are detailed below.

GLMM- Post-Hoc - Estimated Means- Treatment Effects by Plant Community

Regeneration Density

After FDR correction, Pyrophyte density did not differ significantly between treatments in any plant community. Interestingly, burned plots had lower Pyrophyte regeneration on xeric sites (Thermic Oak: ratio = 0.41, 95% CI 0.11–1.56, $p = 0.25$; Mid-slope Oak/Pine: ratio = 0.61, 95% CI 0.19–1.91, $p = 0.43$) and slightly higher regeneration on mesic sites (Bottomland/Cove: ratio = 1.47, 95% CI 0.38–5.64, $p = 0.58$), but none of these patterns were statistically reliable. Pyrophobe density increased significantly in burned plots across Mid-slope Oak/Pine (ratio = 5.56, 95% CI 2.39–12.95, $p < 0.001$) and Thermic Oak communities (ratio = 7.73, 95% CI 2.66–22.45, $p < 0.001$). Bottomland/Cove showed as weaker trend (ratio = 3.03, 95% CI 1.02–9.01, $p = 0.08$). (Fig. 2.4; Appendix B, Table B2).

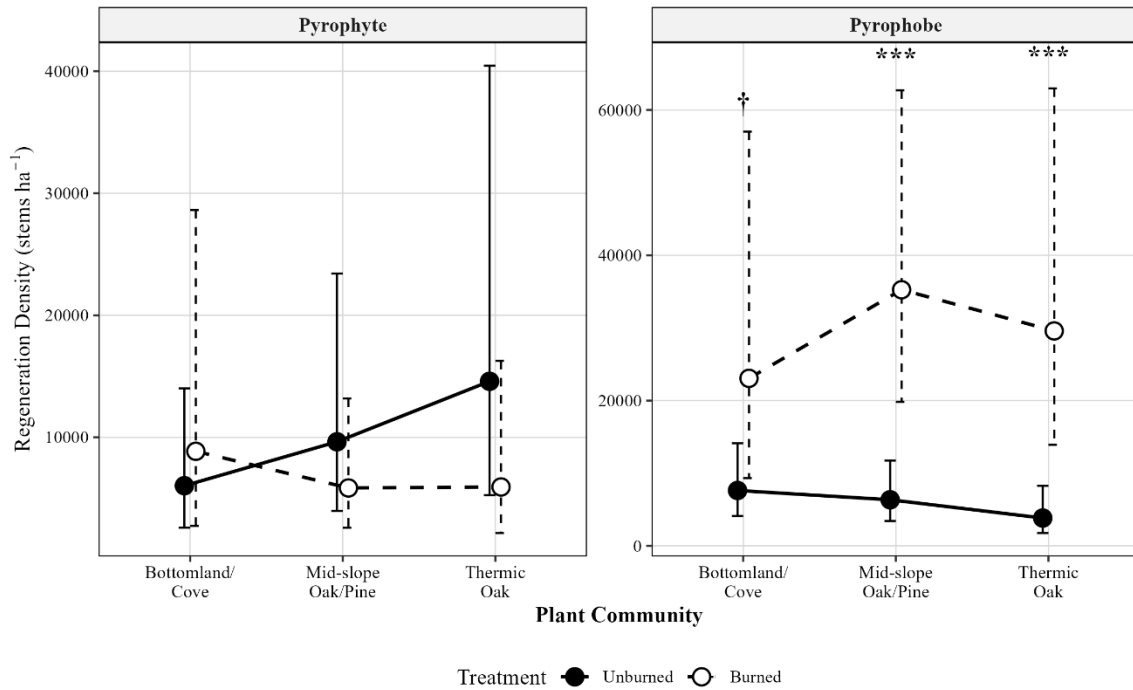


Fig. 2.4. Regeneration density by species group and plant community following the 2016 Rock Mountain Fire. Closed circles represent unburned plots and open circles represent burned plots. Points show mean density ($\pm 95\%$ CI). Pyrophobic species show statistically significantly elevated regeneration in burned Mid-slope Oak/Pine and Thermic Oak communities (***) ($p < 0.001$), while pyrophytic regeneration did not differ by treatment.

Relative Abundance

Wildfire effects reduced Pyrophyte relative abundance in Thermic Oak communities (odds ratio = 0.09, 95% CI 0.03–0.24, $p < 0.001$). Mid-slope Oak/Pine showed a small decrease (odds ratio = 0.46, 95% CI 0.22–0.97, $p = 0.08$), while Bottomland/Cove showed no significant change (odds ratio = 0.53, 95% CI 0.20–1.43, $p = 0.25$).

Pyrophobe relative abundance shows that significant increases occurred in both Mid-slope Oak/Pine (odds ratio = 4.24, 95% CI 1.99–9.01, $p < 0.001$) and Thermic Oak communities (odds ratio = 5.42, 95% CI 2.13–13.81, $p < 0.001$). Bottomland/Cove trended similarly but did not reach significance (odds ratio = 1.88, 95% CI 0.73–4.84, $p = 0.25$) (Fig. 2.5)

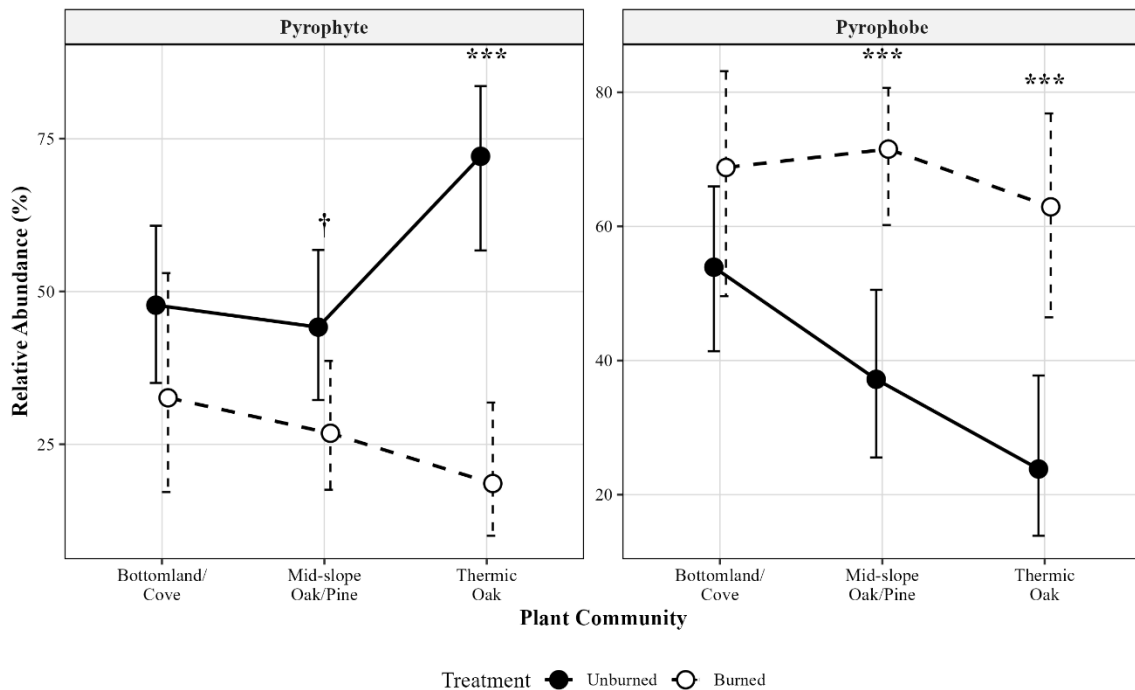


Fig. 2.5. Relative abundance of regeneration by functional group and plant community following the 2016 Rock Mountain Fire. Closed circles represent unburned plots, open circles represent burned plots. Points show mean relative abundance ($\pm 95\%$ CI). Fire significantly decreased pyrophytic dominance in Thermic Oak communities and pyrophobic relative abundance was significantly elevated in burned Mid-slope and Thermic Oak sites. Note: *** $p < 0.001$

DISCUSSION

Forest Regeneration Patterns Post-Wildfire

Drought-induced wildfire effects on regeneration differ by topographic orientation, with strongest pyrophyte response in historically fire-maintained plant communities.

The 91% decline in odds of pyrophyte relative abundance in burned Thermic Oak plots contradicts previous research conducted on pyrophyte regeneration on fire-adapted forests and plant communities (Hagan et al. 2015; Abrams 1992; Brose et al. 2013). The non-significant Treatment \times Group interaction indicates pyrophytes failed to increase relative to other groupings following wildfire, despite fire-adapted traits (Arthur et al. 2012). This pattern was most pronounced in Thermic Oak communities, historically fire-maintained systems where pyrophyte recovery is expected (Hagan et al. 2015). This may be due to resilience debt, a diminished capacity of ecological systems to recover from disturbance following a long break from historical disturbance regime (Taylor et al. 2025; Johnstone et al. 2016). Additionally, the significant increases in pyrophobe relative abundance on site suggest that a single wildfire event in the Southern Appalachian Mountains is insufficient to reverse mesophication compositional trends (Nowacki & Abrams, 2008) and is in fact emerging evidence supporting drought-induced fire effects accelerating mesophication.

It is important to note that fire impacts between wildfire and prescribed fire are different. Prescribed fire occurs under much lower KDBI values and therefore behaves differently (Addington et al. 2015). Prescribed fire rarely results in long-term smoldering, and duff often does not burn at all due to higher moisture conditions at the time of ignition (Varner et al. 2009; Kreye et al. 2020). Additionally, prescribed fire is more constrained by topography in the southern Appalachians, where northeast slopes may not burn well, if at all due to moisture influences on fuels (Vaughan et al. 2021). In contrast, drought conditions prior to the majority of the 2016 wildfires resulted in fire spread across the entire landscape, including normally moist aspects and topographic positions that would typically inhibit prescribed burning (Reilly et al. 2022).

The significant effect of Heat Load Index for this study suggests that site-level environmental stress conditions influence regeneration outcomes, with pyrophyte declines most pronounced on high solar radiation sites. Carpenter et al.'s (2021) work concludes how decades of fire exclusion may have altered these systems in ways that made them vulnerable to wildfire impacts. The drivers of pyrophyte regeneration failure in this study remain unclear and warrant further investigation in future research, including studies assessing regeneration response of pyrophytes and pyrophobes and the link between underground and above ground drivers.

Climate Context and Management Implications

The 2016 fire events burned more area than the previous three decades combined (Reilly et al. 2022), during the likely most severe fall drought on record in the southern Appalachians (Williams et al. 2013). Climate projections suggest drought stress conditions that favored the 2016 wildfire events are likely to increase. Robbins et al. (2024) projects a 10 to 42 percent increase in burned area of eastern temperate forests, depending on drought scenario.

Limitations and Conclusions

Limitations for this study include an absence of pre-fire baseline data, a single fire event, and no direct fire severity covariate, seasonality, and physiological factors. Season of ignition and combustion may influence regeneration outcomes. This study's wildfire occurred in Fall; however seasonality may influence regeneration. These seasonal differences may directly influence regeneration patterns following wildfire and need further investigation.

Established midstory and understory are likely also important factors in recruitment patterns. Stand basal area was not incorporated in this study and could be.

Additionally, this study represents a single fire event, and historical fire regimes in the region were characterized by repeated, mixed-severity burns that progressively suppresses mesophytic competition where a high severity fire such as the 2016 drought-induced Rock Mountain Fire would initially knock out large diameter overstory species,

decreasing basal area and increasing recruitment potential for all species. With historic fire regimes, low-moderate intensity fires would then reduce competition, which does not typically occur at wildfire sites (Aldrich et al., 2010). Decades of fire suppression have permitted shade-tolerant mesophytic species to establish in the midstory and understory where they would not otherwise persist, altering post-fire regeneration. These data suggest that, without prescribed fire or focused restoration efforts prior to wildfire occurrence, a single wildfire event may accelerate mesophication in the Southern Appalachians. Further research across multiple fire events and seasons is needed to fully characterize wildfire's role in mesophication dynamics across the region.

LITERATURE CITED

- Abrams, M. D. (1992). Fire and the development of oak forests. *BioScience*, 42(5), 346–353. <https://doi.org/10.2307/1311781>
- Alexander, H. D., & Arthur, M. A. (2014). Increasing red maple leaf litter alters decomposition rates and nitrogen cycling in historically oak-dominated forests of the eastern U.S. *Ecosystems*, 17(8), 1371–1383. <https://doi.org/10.1007/s10021-014-9802-4>
- Anthropic. (2026). Claude (Claude Opus 4.6) Large language model. <https://claude.ai>
- Arthur, M. A., Alexander, H. D., Dey, D. C., Schweitzer, C. J., & Loftis, D. L. (2012). Refining the oak-fire hypothesis for management of oak-dominated forests of the eastern United States. *Journal of Forestry*, 110(5), 257–266. <https://doi.org/10.5849/jof.11-080>
- Arthur, M. A., Varner, J. M., Lafon, C. W., Alexander, H. D., Dey, D. C., Harper, C. A., Horn, S. P., Hutchinson, T. F., Keyser, T. L., Lashley, M. A., Moorman, C. E., & Schweitzer, C. J. (2021). Fire ecology and management in eastern broadleaf and Appalachian forests. In C. H. Greenberg & B. Collins (Eds.), *Fire ecology and management: Past, present, and future of US forested ecosystems* (pp. 105–147). Springer International Publishing. https://doi.org/10.1007/978-3-030-73267-7_4
- Beasley, C., Carter, D. R., Coates, T. A., Keyser, T. L., & Greenberg, C. H. (2022). Impacts of oak-focused silvicultural treatments on the regeneration layer nine

- years posttreatment in a productive mixed-oak southern Appalachian forest. *Journal of the Torrey Botanical Society*, 149(2), 117–133.
- Beck, H., Zimmermann, N., McVicar, T., Vergopolan, N., Berg, A., & Wood, E. F. (2018). Present and future Köppen-Geiger climate classification maps at 1-km resolution. *Scientific Data*, 5, 180214. <https://doi.org/10.1038/sdata.2018.214>
- Benjamini, Y., & Hochberg, Y. (1995). Controlling the false discovery rate: A practical and powerful approach to multiple testing. *Journal of the Royal Statistical Society: Series B (Methodological)*, 57(1), 289–300. <https://doi.org/10.1111/j.2517-6161.1995.tb02031.x>
- Bolker, B. M., Brooks, M. E., Clark, C. J., Geange, S. W., Poulsen, J. R., Stevens, M. H. H., & White, J.-S. S. (2009). Generalized linear mixed models: A practical guide for ecology and evolution. *Trends in Ecology & Evolution*, 24(3), 127–135. <https://doi.org/10.1016/j.tree.2008.10.008>
- Bray, J. R., & Curtis, J. T. (1957). An ordination of the upland forest communities of southern Wisconsin. *Ecological Monographs*, 27(4), 326–349. <https://doi.org/10.2307/1942268>
- Brooks, M., Kristensen, K., Benthem, K., Magnusson, A., Berg, C., Nielsen, A., Skaug, H., Mächler, M., & Bolker, B. (2017). glmmTMB balances speed and flexibility among packages for zero-inflated generalized linear mixed modeling. *The R Journal*, 9(2), 378. <https://doi.org/10.32614/RJ-2017-066>
- Brose, P. H., Dey, D. C., Phillips, R. J., & Waldrop, T. A. (2013). A meta-analysis of the fire-oak hypothesis: Does prescribed burning promote oak reproduction in eastern

- North America? *Forest Science*, 59(3), 322–334.
<https://doi.org/10.5849/forsci.12-039>
- Brose, P. H., Dey, D. C., & Waldrop, T. A. (2014). *The fire-oak literature of eastern North America: Synthesis and guidelines* (Gen. Tech. Rep. NRS-135). U.S. Department of Agriculture, Forest Service, Northern Research Station.
- Carpenter, D. O., Taylor, M. K., Callaham, M. A., Jr., Hiers, J. K., Loudermilk, E. L., O'Brien, J. J., & Wurzbarger, N. (2020). Benefit or liability? The ectomycorrhizal association may undermine tree adaptations to fire after long-term fire exclusion. *Ecosystems*, 23(2), 369–383.
- Carpenter, D. O., Taylor, M. K., Callaham, M. A., Jr., Hiers, J. K., Loudermilk, E. L., O'Brien, J. J., & Wurzbarger, N. (2021). Benefit or liability? The ectomycorrhizal association may undermine tree adaptations to fire after long-term fire exclusion. *Ecosystems*, 24(5), 1059–1074. <https://doi.org/10.1007/s10021-020-00568-7>
- Clarke, K. R. (1993). Non-parametric multivariate analyses of changes in community structure. *Australian Journal of Ecology*, 18(1), 117–143.
<https://doi.org/10.1111/j.1442-9993.1993.tb00438.x>
- Dey, D. C., & Kabrick, J. M. (2016). Fire in eastern North American oak ecosystems: Filling the gaps. *Fire Ecology*, 12(2), 1–6.
<https://doi.org/10.4996/fireecology.1202001>
- Donovan, V. M., Crandall, R., Fill, J., & Wonkka, C. L. (2023). Increasing large wildfire in the eastern United States. *Geophysical Research Letters*, 50(24), e2023GL107051. <https://doi.org/10.1029/2023GL107051>

- Douma, J. C., Weedon, J. T., & Warton, D. (2019). Analysing continuous proportions in ecology and evolution: A practical introduction to beta and Dirichlet regression. *Methods in Ecology and Evolution*, *10*(9), 1412–1430.
<https://doi.org/10.1111/2041-210X.13234>
- Edwards, L. (Eds.), Kirkman, L. K., & Ambrose, J. (2013). *The natural communities of Georgia*. <https://www.naturalcommunitiesofgeorgia.com/>
- Esri. (2024, December). *USA Soils Map Units* (Feature layer). USDA NRCS, Esri.
<https://www.arcgis.com/home/item.html?id=06e5fd61bdb6453fb16534c676e1c9b9>
- Fei, S., Kong, N., Steiner, K. C., Moser, W. K., & Steiner, E. B. (2011). Change in oak abundance in the eastern United States from 1980 to 2008. *Forest Ecology and Management*, *262*(8), 1370–1377. <https://doi.org/10.1016/j.foreco.2011.06.030>
- Flatley, W. T., Lafon, C. W., Grissino-Mayer, H. D., & LaForest, L. B. (2013). Fire history, related to climate and land use in three southern Appalachian landscapes in the eastern United States. *Ecological Applications*, *23*(6), 1250–1266.
<https://doi.org/10.1890/12-1752.1>
- Fox, J., & Weisberg, S. (2019). *An R companion to applied regression* (3rd ed.). Sage.
<https://socialsciences.mcmaster.ca/jfox/Books/Companion/>
- Gaffin, D., & Hotz, D. (2000). A precipitation and flood climatology with synoptic features of heavy rainfall across the southern Appalachian Mountains. *National Weather Digest*, *24*, 3–15.

- Griffith, G. E., Omernik, J. M., Comstock, J. A., Lawrence, S., Martin, G., Goddard, A., Hulcher, V. J., & Foster, T. (2001). *Ecoregions of Alabama and Georgia* [Map]. U.S. Geological Survey.
- Hagan, D. L., Waldrop, T. A., Reilly, M., & Shearman, T. M. (2015). Impacts of repeated wildfire on long-unburned plant communities of the southern Appalachian Mountains. *International Journal of Wildland Fire*, 24(7), 911–920.
<https://doi.org/10.1071/WF14143>
- Hartig, F. (2022). *DHARMA: Residual diagnostics for hierarchical (multi-level/mixed) regression models* (R package version 0.4.6). <https://CRAN.R-project.org/package=DHARMA>
- Harper, C. A., Ford, W. M., Lashley, M. A., Moorman, C. E., & Stambaugh, M. C. (2016). Fire effects on wildlife in the Central Hardwoods and Appalachian regions, USA. *Fire Ecology*, 12(2), 127–159.
<https://doi.org/10.4996/fireecology.1202127>
- Hutchinson, T. F., Long, R. P., Ford, R. D., & Sutherland, E. K. (2008). Fire history and the establishment of oaks and maples in second-growth forests. *Canadian Journal of Forest Research*, 38(5), 1184–1198. <https://doi.org/10.1139/X07-216>
- Hutchinson, T. F., Adams, B. T., Dickinson, M. B., & Thomas-Van Gundy, M. A. (2024). Sustaining eastern oak forests: Synergistic effects of fire and topography on vegetation and fuels. *Ecological Applications*, 34(3), e2948.
<https://doi.org/10.1002/eap.2948>

- Iverson, L. R., Hutchinson, T. F., Peters, M. P., & Yaussy, D. A. (2017). Long-term response of oak-hickory regeneration to partial harvest and repeated fires: Influence of light and moisture. *Ecosphere*, *8*(1), e01642.
- Jenks, G. F. (1967). The data model concept in statistical mapping. *International Yearbook of Cartography*, *7*, 186–190.
- Johnstone, J. F., Allen, C. D., Franklin, J. F., Frelich, L. E., Harvey, B. J., Higuera, P. E., Mack, M. C., Meentemeyer, R. K., Metz, M. R., Perry, G. L. W., Schoennagel, T., & Turner, M. G. (2016). Changing disturbance regimes, ecological memory, and forest resilience. *Frontiers in Ecology and the Environment*, *14*(7), 369–378.
<https://doi.org/10.1002/fee.1311>
- Keyser, T. L. (2019). Resprouting by seedlings of four North American deciduous broadleaved tree species following experimental burning. *Oecologia*, *190*(1), 207–218. <https://doi.org/10.1007/s00442-019-04397-x>
- Keyser, T. L., Arthur, M. A., & Loftis, D. L. (2017). Repeated burning alters the structure and composition of hardwood regeneration in oak-dominated forests of eastern Kentucky, USA. *Forest Ecology and Management*, *393*, 1–11.
<https://doi.org/10.1016/j.foreco.2017.03.015>
- Keyser, T. L., Greenberg, C. H., & McNab, W. H. (2019). Season of burn effects on vegetation structure and composition in oak-dominated Appalachian hardwood forests. *Forest Ecology and Management*, *433*, 441–452.
- Kruskal, J. B. (1964). Nonmetric multidimensional scaling: A numerical method. *Psychometrika*, *29*(2), 115–129. <https://doi.org/10.1007/BF02289694>

- Lafon, C. W., Naito, A. T., Grissino-Mayer, H. D., Horn, S. P., & Waldrop, T. A. (2017). *Fire history of the Appalachian region: A review and synthesis* (General Technical Report SRS-219). U.S. Department of Agriculture, Forest Service, Southern Research Station.
- Legge, E. O. L., Koyama, A., Fernandez, C. W., Wood, K. E. A., Triviño Silva, N. J., Brudvig, L. A., & Vander Yacht, A. L. (2025). Dearth under earth: Understudied plant-soil-fire feedback as drivers of forest mesophication and oak regeneration failures. *Forest Ecology and Management*, 597, 123147. <https://doi.org/10.1016/j.foreco.2025.123147>
- Lenth, R. V. (2024). *emmeans: Estimated marginal means, AKA least-squares means* (R package version 1.10.0). <https://CRAN.R-project.org/package=emmeans>
- Lorimer, C. G., Chapman, J. W., & Lambert, W. D. (1994). Tall understorey vegetation as a factor in the poor development of oak seedlings beneath mature stands. *The Journal of Ecology*, 82(2), 227–237. <https://doi.org/10.2307/2261291>
- McCune, B., & Keon, D. (2002). Equations for potential annual direct incident radiation and heat load. *Journal of Vegetation Science*, 13(4), 603–606.
- McCune, B. (2007). Improved estimates of incident radiation and heat load using non-parametric regression against topographic variables. *Journal of Vegetation Science*, 18(5), 751–754. <https://doi.org/10.1111/j.1654-1103.2007.tb02590.x>
- McEwan, R. W., Hutchinson, T. F., Long, R. P., Ford, D. R., & McCarthy, B. C. (2007). Temporal and spatial patterns in fire occurrence during the establishment of

- mixed-oak forests in eastern North America. *Journal of Vegetation Science*, 18(5), 655–664. <https://doi.org/10.1111/j.1654-1103.2007.tb02579.x>
- McShea, W. J., Healy, W. M., Devers, P., Fearer, T., Koch, F. H., Stauffer, D., & Waldon, J. (2007). Forestry matters: Decline of oaks will impact wildlife in hardwood forests. *Journal of Wildlife Management*, 71(5), 1717–1728. <https://doi.org/10.2193/2006-169>
- NEON (National Ecological Observatory Network). (2021). *TOS Protocol and Procedure: Measurement of Vegetation Structure*. NEON Doc. #: NEON.DOC.000987. Available at: <https://data.neonscience.org/>
- NOAA National Centers for Environmental Information. (2025, January). *Climate at a glance: County time series*. <https://www.ncei.noaa.gov/access/monitoring/climate-at-a-glance/county/time-series>
- North, M. A. (2009). A method for implementing a statistically significant number of data classes in the Jenks algorithm. In *The Sixth International Conference on Fuzzy Systems and Knowledge Discovery: Proceedings, Tianjin, China, 14–16 August 2009* (Vol. 1, pp. 35–38). <https://doi.org/10.1109/FSKD.2009.319>
- Nowacki, G. J., & Abrams, M. D. (2008). The demise of fire and “mesophication” of forests in the eastern United States. *BioScience*, 58(2), 123–138.
- Oakman, E. C., Hagan, D. L., Waldrop, T. A., & Barrett, K. (2021). Understory community shifts in response to repeated fire and fire surrogate treatments in the

- southern Appalachian Mountains, USA. *Fire Ecology*, 17(1), Article 7.
<https://doi.org/10.1186/s42408-021-00097-1>
- Oksanen, J., Blanchet, F. G., Kindt, R., Legendre, P., McGlinn, D., Minchin, P. R., O'Hara, R. B., Simpson, G. L., Solymos, P., Stevens, M. H. H., Szoecs, E., & Wagner, H. (2024). *vegan: Community ecology package* (R package version 2.7-2). <https://CRAN.R-project.org/package=vegan>
- Palus, J. D., Goebel, P. C., Hix, D. M., & Matthews, S. N. (2018). Structural and compositional shifts in forests undergoing mesophication in the Wayne National Forest, southeastern Ohio. *Forest Ecology and Management*, 430, 413–420.
<https://doi.org/10.1016/j.foreco.2018.08.030>
- Pausas, J. G. (2015). Bark thickness and fire regime. *Functional Ecology*, 29(3), 315–327. <https://doi.org/10.1111/1365-2435.12372>
- Peet, R. K., Wentworth, T. R., & White, P. S. (1998). A flexible, multipurpose method for recording vegetation composition and structure. *Castanea*, 63(3), 262–274.
- R Core Team. (2024). *R: A language and environment for statistical computing*. R Foundation for Statistical Computing. <https://www.R-project.org/>
- Reilly, M. J., Norman, S. P., O'Brien, J. J., & Loudermilk, E. L. (2022). Drivers and ecological impacts of a wildfire outbreak in the southern Appalachian Mountains after decades of fire exclusion. *Forest Ecology and Management*, 524, 120500.
<https://doi.org/10.1016/j.foreco.2022.120500>
- Robbins, Z. J., Loudermilk, E. L., Mozelewski, T. M., Jones, K., & Scheller, R. M. (2024). Fire regimes of the Southern Appalachians may radically shift under

- climate change. *Fire Ecology*, 20, Article 2. <https://doi.org/10.1186/s42408-023-00231-1>
- Seyfried, M., Flerchinger, G., Bryden, S., Link, T., Marks, D., & McNamara, J. (2021). Slope and aspect controls on soil climate: Field documentation and implications for large-scale simulation of critical zone processes. *Vadose Zone Journal*, 20(6). <https://doi.org/10.1002/vzj2.20158>
- Spînu, A. P., Niklasson, M., & Zin, E. (2020). Mesophication in temperate Europe: A dendrochronological reconstruction of tree succession and fires in a mixed deciduous stand in Białowieża Forest. *Ecology and Evolution*, 10(2), 1029–1041. <https://doi.org/10.1002/ece3.5966>
- Taylor, M. K., Hagan, D. L., Coates, T. A., DeFeo, J. A., Callaham, M. A., Mohr, H. H., Waldrop, T. A., & Wurzbarger, N. (2025). Reducing resilience debt: Mechanical felling and repeated prescribed fires may sustain eastern oak forests. *Ecological Applications*, 35(7), e70125-n/a. <https://doi.org/10.1002/eap.70125>
- United States Department of Agriculture, Natural Resources Conservation Service. (2025). *Custom soil resource report for Dawson, Lumpkin, and White Counties, Georgia; Fannin and Union Counties, Georgia; Habersham County, Georgia; and Rabun and Towns Counties, Georgia*. <https://websoilsurvey.sc.egov.usda.gov/>
- U.S. Geological Survey. (2025). *Digital elevation model* [Data set]. Earth Explorer. <https://earthexplorer.usgs.gov/>

- Van Lear, D. H., & Waldrop, T. A. (1989). *History, uses, and effects of fire in the Appalachians* (Gen. Tech. Rep. SE-54). U.S. Department of Agriculture, Forest Service, Southeastern Forest Experiment Station.
- Varner, J. M., Kane, J. M., Hiers, J. K., Kreye, J. K., & Veldman, J. W. (2016). Suites of fire-adapted traits of oaks in the southeastern USA: Multiple strategies for persistence. *Fire Ecology*, *12*(2), 48–64.
<https://doi.org/10.4996/fireecology.1202048>
- Williams, A. P., Cook, B. I., Smerdon, J. E., Bishop, D. A., Seager, R., & Mankin, J. S. (2017). The 2016 southeastern U.S. drought: An extreme departure from centennial wetting and cooling. *Journal of Geophysical Research: Atmospheres*, *122*, 10888–10905.
- Woodbridge, M. E., Keyser, T. L., & Oswalt, C. M. (2022). Stand and environmental conditions drive functional shifts associated with mesophication in eastern US forests. *Forest Ecology and Management*, *517*, 120277.
<https://doi.org/10.1016/j.foreco.2022.120277>
- Zuur, A. F., Ieno, E. N., Walker, N. J., Saveliev, A. A., & Smith, G. M. (2009). *Mixed effects models and extensions in ecology with R*. Springer.
<https://doi.org/10.1007/978-0-387-87458-6>

APPENDICES

Appendix A

Table A1

*Posterior estimates of fire effects on cumulative overstory mortality by functional group from Bayesian hierarchical logistic regression (Model 1). Note: *95% credible interval excludes zero log-odds) and one (OR). Median ORs reported.*

Group	β (log-odds)	β 95% CI	Odds-Ratio	OR 95% CI
Pyrophytic	0.81	-0.3, 1.96	2.2	0.7, 7.1
Pyrophobic	3.85	1.82, 6.39*	43.1	6.2, 598.5
Heath	2.59	1.33, 4.06*	12.8	3.8, 57.9

Table A2

Posterior estimates of interaction effects from Bayesian hierarchical logistic regression (Model 1). Note: $P(>0)$ = posterior probability that parameter is positive.

**95% credible interval excludes zero.*

Parameter	β (log-odds)	β 95% CI	P(>0)
Fire Effect (Pyrophytic)	1.81	-0.77, 4.36	0.92
Fire \times Pyrophobic	2.04	-0.88, 5.10	0.91
Fire \times Heath	0.78	-1.91, 3.50	0.71

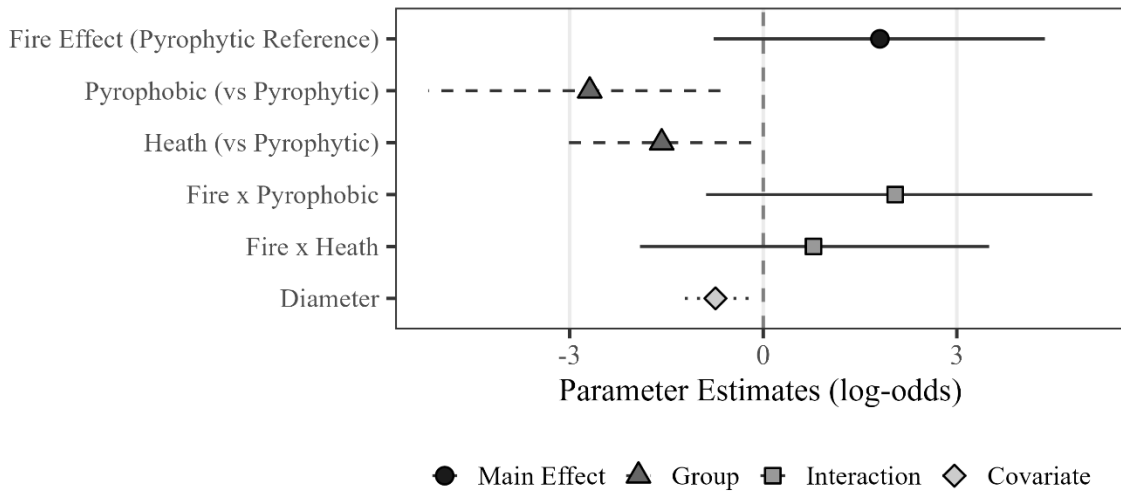


Fig. A1 Forest plot of Model 1 coefficients relative to pyrophytes. Points represent posterior mean log-odds estimates, horizontal lines indicate 95% credible intervals, and the vertical line= line of no effect. Circles = main effects, triangles = group intercepts, squares = Fire × Group interactions, diamonds = covariates. Asterisks = 95% credible intervals excluding zero.

Table A3

Model 2 Descriptive statistics and mortality rate by period and treatment at rock mountain wildfire.

Period	Treatment	Trees (n)	Deaths (n)	Mortality (%)
Early	Unburned	120	6	5.0
	Burned	113	20	17.7
Late	Unburned	114	6	5.3
	Burned	91	28	30.8

Table A4

Model 2 predicted mortality hazard rates by period and treatment from Bayesian hierarchical logistic regression (Model 2).

Period	Treatment	Hazard (%)	95% CI
Early	Unburned	4.3	1.6, 8.5
	Burned	14.4	7.8, 22
Late	Unburned	4.6	1.6, 9.1
	Burned	29	19.1, 40.1

Table A5

Fire effect on mortality hazard by period from Bayesian hierarchical logistic regression (Model 2).

Period	Unburned (%)	Burned (%)	95% CI
Early	4.3	14.4	1.5, 9.2
Late	4.6	29.0	2.9, 18.5

Table A6

Model 2 parameter estimates from Bayesian hierarchical logistic regression. B represents coefficients on the log-odds scale with 95% credible intervals.

Parameter	β (log-odds)	95% CI	$P(\beta > 0)$
Intercept	-3.18	-4.13, -2.38	0.00
Fire Effect	1.36	0.41, 2.38	1.00
Period Effect	0.05	-1.08, 1.18	0.54
Fire \times Period	0.85	-0.45, 2.18	0.90
Diameter	-0.58	-1.01, -0.19	0.00

Table A7

Model-predicted mortality probability (%) across heat load index (HLI) sites from Bayesian hierarchical logistic regression (Model 3). Note: Posterior means at mean diameter.

HLI	Treatment	Mortality (%)	95 CI %
Mesic (HLI = -1)	Unburned	10.1	4.3, 18
Intermediate (HLI = 0)	Unburned	9.1	4.5, 15.1
Xeric (HLI = +1)	Unburned	8.7	2.9, 17.6
Mesic (HLI = -1)	Burned	23.2	11.2, 37.8
Intermediate (HLI = 0)	Burned	35.6	25.2, 46.4
Xeric (HLI = +1)	Burned	50.9	36.5, 65.5

Table A8

Fire effect on mortality across the topographic moisture gradient from Bayesian hierarchical logistic regression (Model 3).

Site Type	Unburned (%)	Burned (%)	95% CI
Mesic (HLI = -1)	10.1	23.2	0.9, 5.9
Intermediate (HLI = 0)	9.1	35.6	2.2, 8.2
Xeric (HLI = +1)	8.7	50.9	2.7, 18.2

Table A9

Model 3 parameter estimates from Bayesian hierarchical logistic regression. β

represents coefficients on the log-odds scale with 95% credible intervals. Note: $P(\beta > 0)$

= posterior probability parameter is positive.

Parameter	Beta	95% CI	P($\beta > 0$)
Intercept	-2.35	-3.07, -1.73	0.0
Fire Effect	1.75	0.98, 2.57	1.0
HLI Effect	-0.1	-0.71, 0.49	0.37
Fire \times HLI	0.74	-0.03, 1.54	0.97
Diameter	-0.57	-1.02, -0.16	0.0

Appendix B

Table B1

Post-hoc pairwise contrasts results of regeneration density at rock mountain study site.

*Note: significant results in **bold**.*

Species Group	PC Grouping	Ratio	CI	P-Value	P-Val (FDR)
Pyrophyte	Bottomland/Cove	1.47	(0.38-5.64)	0.577	0.577
	Mid-slope	0.61	(0.19-1.91)	0.394	0.430
	Oak/Pine				
	Thermic Oak, Oak/Pine	0.41	(0.11-1.56)	0.190	0.250
Pyrophobe	Bottomland/Cove	3.03	(1.02-9.01)	0.047	0.080
	Mid-slope	5.56	(2.39-12.95)	<0.001	<0.001
	Oak/Pine				
	Thermic Oak, Oak/Pine	7.73	(02.66-22.45)	<0.001	<0.001

Table B2*Post-hoc pairwise contrasts results of relative abundance at rock mountain study site.**Note: significant results in **bold**.*

Species Group	PC Grouping	Ratio	CI	P-Value	P-Val (FDR)
Pyrophyte	Bottomland/Cove	0.53	(0.20- 1.43)	0.209	0.250
	Mid-slope	0.46	(0.22- 0.97)	0.042	0.080
	Oak/Pine				
	Thermic Oak, Oak/Pine	0.09	(0.03- 0.24)	<0.001	<0.001
Pyrophobe	Bottomland/Cove	1.88	(0.73- 4.84)	0.189	0.250
	Mid-slope	4.24	(1.99- 9.01)	<0.001	<0.001
	Oak/Pine				
	Thermic Oak, Oak/Pine	5.42	(2.13- 13.81)	<0.001	<0.001